Establishment of Proximity-dependent Biotinylation Approaches in Different Plant Model Systems

Deepanksha Arora[1,2,*], Nikolaj B. Abel[3,*], Chen Liu[4,*], Petra Van Damme[1,2,5,*], Lam Dai Vu[1,2], Anna Tornkvist[4], Francis Impens[6,7,8], Dominique Eeckhout[1,2], Alain Goossens[1,2], Geert De Jaeger[1,2,#], Thomas Ott[3,9,#], Panagiotis Moschou[4,10,11,#], Daniel Van Damme[1,2,#]

[1] Ghent University, Department of Plant Biotechnology and Bioinformatics, Technologiepark 71, 9052 Ghent University, Ghent, Belgium.
[2] VIB Center for Plant Systems Biology, Technologiepark 71, 9052 Ghent, Belgium.
[3] Faculty of Biology, Cell Biology, University of Freiburg, Germany.
[4] Department of Plant Biology, Uppsala BioCenter, Swedish University of Agricultural Sciences and Linnean Center for Plant Biology, Uppsala, Sweden.
[5] Department of Biochemistry and Microbiology, Ghent University, Ghent, Belgium
[6] Department of Biochemistry, Ghent University, Ghent, Belgium.
[7] VIB Center for Medical Biotechnology, Ghent, Belgium.
[8] VIB Proteomics Core, Ghent, Belgium.
[9] CIBSS – Centre for Integrative Biological Signalling Studies, University of Freiburg, Germany
[10] Department of Biology, University of Crete, Heraklion, Greece.
[11] Institute of Molecular Biology and Biotechnology, Foundation for Research and Technology - Hellas, Heraklion, Greece.

* joint first authors
# joint senior and corresponding authors

Running title: Proximity-dependent biotinylation in plants

Abstract

The use of proximity-dependent biotin labelling (PDL) approaches coupled with mass spectrometry recently greatly advanced the identification of protein-protein interactions and study of protein complexation. PDL is based on the expression of a promiscuous biotin ligase (PBL), e.g. BirA* or a peroxidase fused to a bait protein of interest. In the presence of biotin as substrate, PBL enables covalent biotin labelling of proteins in the vicinity of the PBL-fused bait *in vivo*, allowing the subsequent capture and identification of interacting and neighbouring proteins without the need for the protein complex to remain intact during purification. To date, PDL has not been extensively used in plants. Here we present the results of a systematic multi-lab study applying a variety of PDL approaches in several plant systems under various conditions and bait proteins. We show that TurboID is the most promiscuous variant for PDL in plants and establish protocols for its efficient application. We demonstrate the applicability of TurboID in capturing membrane protein interactomes using the *Lotus japonicus* symbiotically active receptor kinases RLKs NOD FACTOR RECEPTOR 5 (NFR5) and LRR-RLK SYMBIOTIC RECEPTOR-KINASE (SYMRK) as test-cases. Furthermore, we benchmark the efficiency of various PBLs using the octameric endocytic TPLATE complex and compare PDL with one-step AP-MS approaches. Our results indicate that different PDL approaches in plants may differ in signal-to-noise ratio and robustness. We present a straightforward strategy to identify both non-biotinylated as well as biotinylated proteins in plants in a single experimental setup. Finally, we provide initial evidence that this technique has potential to infer structural information of protein complexes. Our methods, tools and adjustable pipelines provide a useful resource for the plant research community.

INTRODUCTION

Protein-protein interaction (PPI) studies often fail to capture low affinity interactions as these are usually not maintained following cell lysis and protein extraction. This is in particular the case for PPI's with or among integral membrane proteins because of the harsh conditions during protein extraction and purification. Proximity-dependent biotin labelling (PDL) on the contrary, uses covalent biotinylation of proteins that are interactors or near-neighbours of a certain bait protein *in vivo* [1]. Hence, in order to identify interactions, they do not need to remain intact during purification. Biotin is an essential cofactor for a small number of omnipresent biotin-dependent enzymes involved mainly in the transfer of CO_2 during HCO_3^--dependent carboxylation reactions. Biotinylation is therefore a relatively rare *in vivo* protein modification. Moreover, biotinylated proteins can be selectively isolated with high avidity using streptavidin-biotin pairing. PDL therefore permits the identification of both high and low affinity interactions.

Analogues to DamID in which a prokaryotic *Dam* methylase is fused to a protein of interest to monitor DNA-protein interactions in eukaryotes [2], the principle of PDL allows the capture of protein-protein interactions. More specifically, PDL is based on the fact that native biotin ligases, e.g. the *Escherichia coli* BirA catalyzes a two-step reaction: first, the generation of reactive biotinyl-AMP (biotinoyl-5'-AMP or bioAMP) from biotin and ATP, and second, the attachment of that bioAMP to a specific lysine of the target protein. Engineered PBLs have a significantly reduced affinity for the reactive bioAMP intermediate [3, 4]. This intermediate is prematurely released and, due to its high reactivity, will interact with neighbouring primary amines (e.g., lysine). Therefore, these variants lead to promiscuous labelling despite their lower affinity for biotin compared to native biotin ligases.

There are several variations of PDL. The first-generation enzymes used for PDL are based on the *E. coli* biotin ligase BirA [5]. The mutant BirA, designated BirA* (R118G) [6], referred hereafter as BioID, a monomeric protein of 35.3 kDa, was the first PBL variant used for PDL [3, 4, 7]. A second-generation PBL, called BioID2, was derived from the *Aquifex aeolicus* biotin ligase [3]. BioID2, which naturally lacks a DNA-binding domain, is approximately one-third smaller than BioID, potentially reducing sterical hindrance of the bait protein [8]. The third-generation PBLs, called TurboID and mini TurboID (mTurboID), are derived from directed evolution of BirA* expressed in yeast. These two variants showed maximal activity at 30^{o}C, while the previous variants show maximal activity at higher temperatures [9]. TurboID has the same size as the original BirA* tag, albeit with 14 amino acid mutations that greatly increase its labelling efficiency. mTurbo has 12 out of 14 of those

mutations. The N-terminal DNA-binding domain was deleted to reduce its size (28 versus 35 kDa), which also slightly impacted on its labelling efficiency by reducing it ~2-fold. The first and second-generation PBLs required approximately 18 to 24 h of labelling (and sometimes even much longer) to produce detectable levels of protein biotinylation, while the TurboID variants required a labelling time only in the range of 1 h or less in the various eukaryotic, non-plant systems tested so far [9].

PDL has its own intrinsic advantages and limitations. In the presence of biotin, the bait-PBL fusion protein labels proximal proteins without the activation by a conditional trigger, thereby keeping track of all interactions that occurred over a time-period. The ability for selective capture makes the method generally insensitive to protein solubility or protein complexation, with obvious applicability to membrane proteins and cytoskeletal constituents, a major advantage over alternative approaches. Nevertheless, the identity of a candidate interactor does not immediately imply a direct or indirect interaction with the bait but could merely reflect close proximity [estimated to be ~10 to 15 nm [10]]. Furthermore, true interactors (false negatives) are missed if they lack accessible primary amines.

So far PBLs have successfully been used in yeast [11], protozoa [12], amoebae [13], embryonic stem cells [14], and xenograft tumors [15] to map a wide range of interactomes in both small-scale (i.e. single bait protein) and large-scale network mapping approaches (i.e. the protein interaction landscape of the centrosome-cilium interface and the organization of mRNA-associated granules and bodies (mRNP complexes)) [16, 17].

In plants, PBLs have not been extensively used. So far, four papers describe the application of PDL in plants [18-21]. In these first trials, overexpression of a first-generation BirA* was used combined with long labelling times, very high biotin levels and relatively poor labelling efficiencies. These results, combined with the so far non-extensive use of PDL in plants could suggest that BioID variants used so far show reduced activity in plant tissues due to suboptimal working temperatures with reference to their temperature-activity profiles.

Here, we report a systematic multi-lab study of different PDL approaches in various plant systems. We provide guidelines for the use of PDL in various frequently used plant models suggesting most relevant shortcomings and contingencies. Furthermore, we benchmark our PDL methods studying the TPLATE protein complex. We foresee that the methods, tools and produced materials will greatly benefit the research community.

RESULTS

Increased PBL-mediated biotin labelling efficiencies upon biotin administration in planta

In non-plant systems, supplementation of biotin is important for efficient proximity biotin ligation with all the PBLs tested so far. In contrast, plants synthesize biotin endogenously and thus the intracellular pool of biotin might be high enough for the PBL. In fact, free biotin has been shown to accumulate in the cytosol of plant mesophyll cells to a high concentration of ca. 11 µM [22], while for example in yeast this is more than 10-fold lower [23]. Considering that

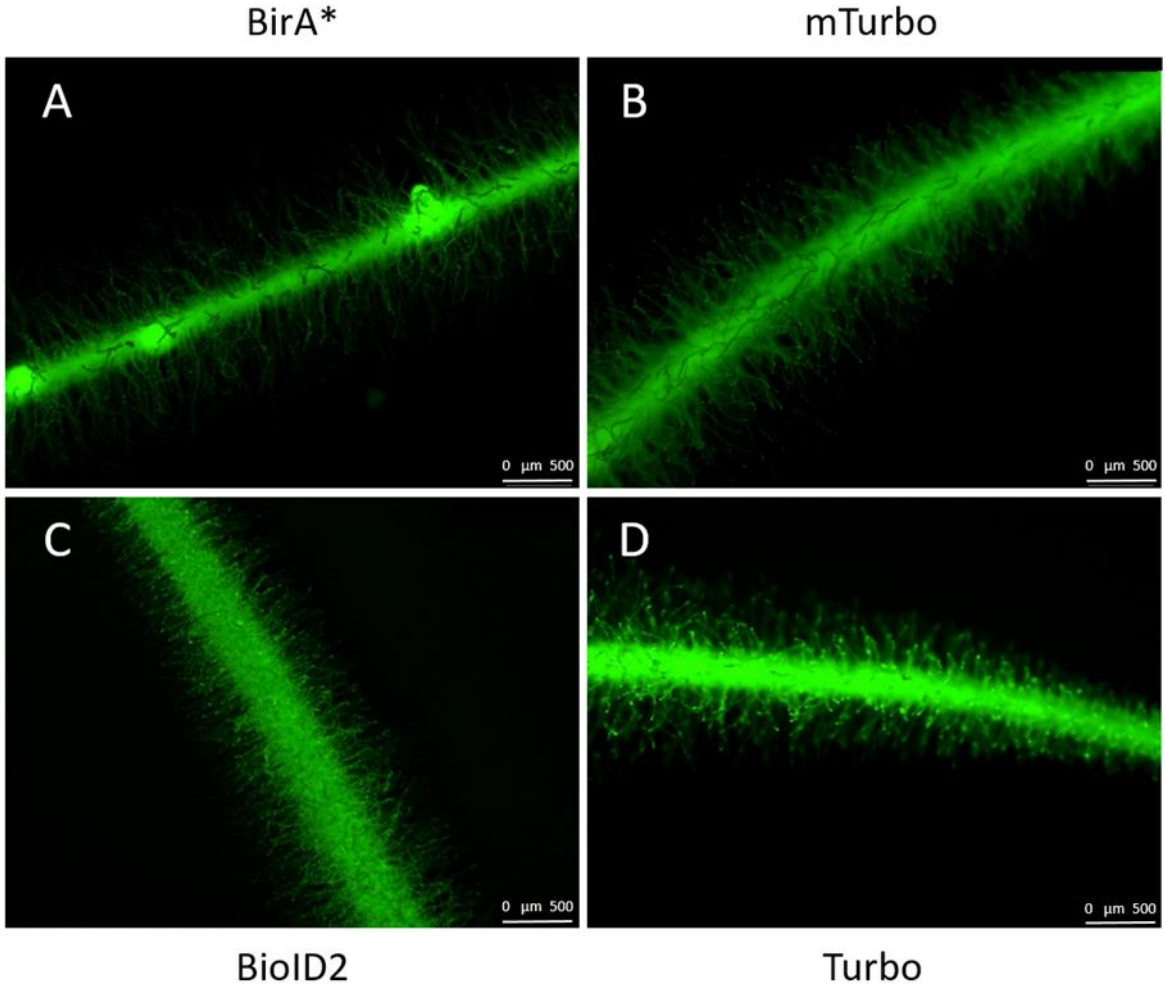

Figure S1. GFP expression in tomato hairy root cultures produced with rhizogenic *Agrobacterium*. Fluorescence micrograph images of eGFP expression were obtained from primary hairy roots (~14 days) transformed rhizogenic *Agrobacterium* with the following expression constructs; Pro35S::eGFP-BirA*, Pro35S::eGFP-BioID2, Pro35S::eGFP-TurboID, and Pro35S::eGFP-miniTurboID. The scale bars are 500 µm. Images are representative for the four to ten independent roots selected for subcultivation and showing expression of the marker per construct.

the K_m of BirA* for biotin is 0.3 µM, this could, in theory, lead to efficient PDL even in the absence of exogenous biotin supplementation.

We thus tested biotinylation efficiency in the presence or absence of biotin using different tagged PBLs as fusion proteins, either codon-optimized for plants or non-codon optimized (**Supplemental Table 1 and Supplemental File 1**). More specifically, we comparatively screened the potential applicability of enzyme-catalyzed proximity labelling when using the PBL BirA* [5, 8], BioID2 [8], TurboID or mTurboID [9]. We first tested these

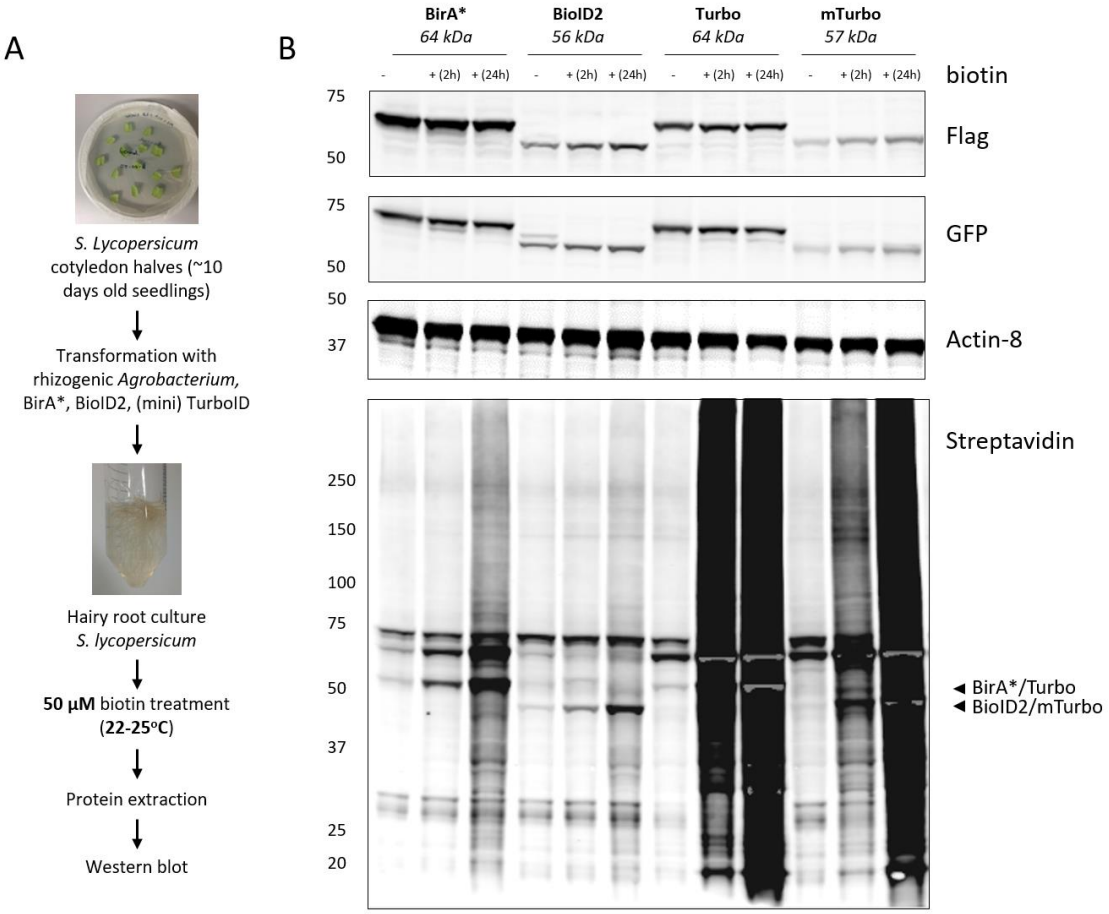

Figure 1. Characterization of enzyme-catalysed proximity labelling in hairy root cultures. (A) Experimental setup. (B) Comparison of biotinylation activity in four PBL-expressing hairy root cultures. Addition of 50 µM exogenous biotin to two-weeks old hairy root cultures for 2 or 24 h was used for labelling. Arrowheads indicate the expected size of the cis-biotinylation signal. (B) Comparison of biotinylation activity in four PBL hairy root cultures from wild-type tomato expressing eGPF.BirA* (~66 kDa), eGPF.BioID2 (~56 kDa), eGPF.Turbo (~64 kDa) and eGPF.miniTurbo (~57 kDa). Gray regions in intense black areas represent saturation of the streptavidin-s680 signal and is most prominent in case of self-biotinylation activity. This is a representative experiment repeated twice and two independent root cultures were analyzed per combination.

PBLs in stable hairy root lines of *Solanum lycopersicum* (see **Materials and Methods**). For protein visualisation, we fused the engineered PBL to FLAG and enhanced green fluorescent protein (eGFP) under control of the constitutive cauliflower mosaic virus (CaMV) 35S promoter (**Supplemental Figure 1**).

As a control for non-bait specific biotinylation, PBL-fused eGFP was used. Biotinylation, was evident as smears in streptavidin-HRP Western blot. This smear depicts biotinylation of other proteins than PBLs, and will be referred to as "trans-biotinylation". As a proxy of PBL activity, we used the cis-biotinylation efficiency (i.e. auto- or self-biotinylation level of PBL fusions) as readout (**Figure 1**). Manifold faster kinetics for TurboID and mTurboID over BioID and BioID2 could be observed (**Figure 1**). This is in line with the previously reported lower catalytic activities of the latter PBLs, especially at the growth conditions used (i.e. cultivation of hairy roots was performed at 22-25°C) [9]. Noteworthy, only residual trans-biotinylation was observed when no exogenous biotin was added. Therefore, the addition of surplus of (free) biotin seems to function as an inducing agent of PDL in this system. This observation indicates that PDL in plants to some extend might also have the capacity to identify the spatiotemporal dynamics of interactome composition.

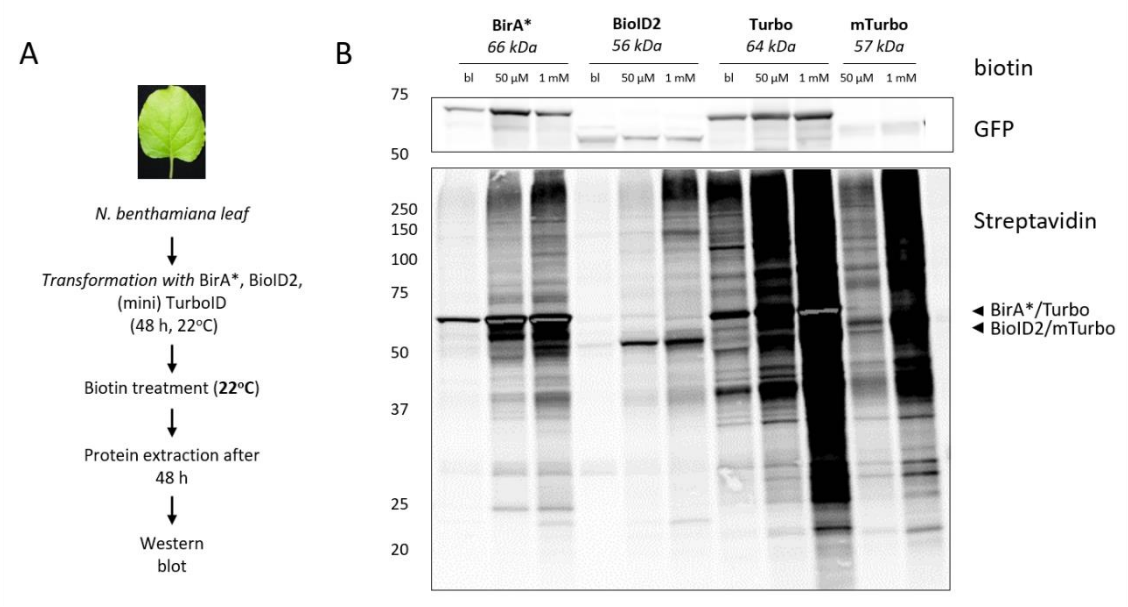

Figure S2 Characterization of PBL-catalysed proximity labelling in *N. benthamiana*. (A) Experimental setup. (B) Comparison of biotinylation activity in *N. benthamiana* expressing eGPF.-BirA* (~66 kDa), eGPF-BioID2 (~56 kDa), eGPF-Turbo (~64 kDa) and eGPF-miniTurbo (~57 kDa). Overlapping signal as indicated with a black arrow denote enzyme-catalysed cis-biotinylation. Gray bands in intense black areas represent saturation of the streptavidin-s680 signal and is most prominent in case of auto-biotinylation activity. Two infiltrated tobacco leaf segments/leaves were analyzed per setup and the experiment was repeated twice with similar results.

PDL-efficiency depends on growth temperatures and PBL can facilitate trans-biotinylation in Nicotiana benthamiana

We used transient transformation of *Nicotiana benthamiana* leaf mesophyll cells to test the applicability of PBL in an alternative system commonly used for protein expression *in planta*

under various conditions. In this case, biotin was infiltrated directly into leaf tissue 24 h after transfection and harvested 24 h post-biotin infiltration (**Supplemental Figure 2A**). We confirmed that also in this system, the highest cis-biotinylation level was observed in the case of TurboID, and supplementation of biotin was important for the efficient detection of cis-biotinylation (**Supplemental Figure 2B**). Furthermore, the overall biotinylation output in tobacco leaves increased when biotin concentration increased from 50 µM to 1 mM (**Supplemental Figure 2B**).

We confirmed that the R118G mutation is responsible for promiscuous labelling in plants, as the wild-type BirA showed no trans-biotinylation (in the presence of 50 µM exogenous biotin; **Supplemental Figure 3A**). Furthermore, a temperature shift from 22°C to 28°C increased cis- and *trans*-biotinylation for both BioID and TurboID, suggesting that temperature control, at least to some extent, could also be used to modulate PDL in plants (**Supplemental Figure 3A**, see also below).

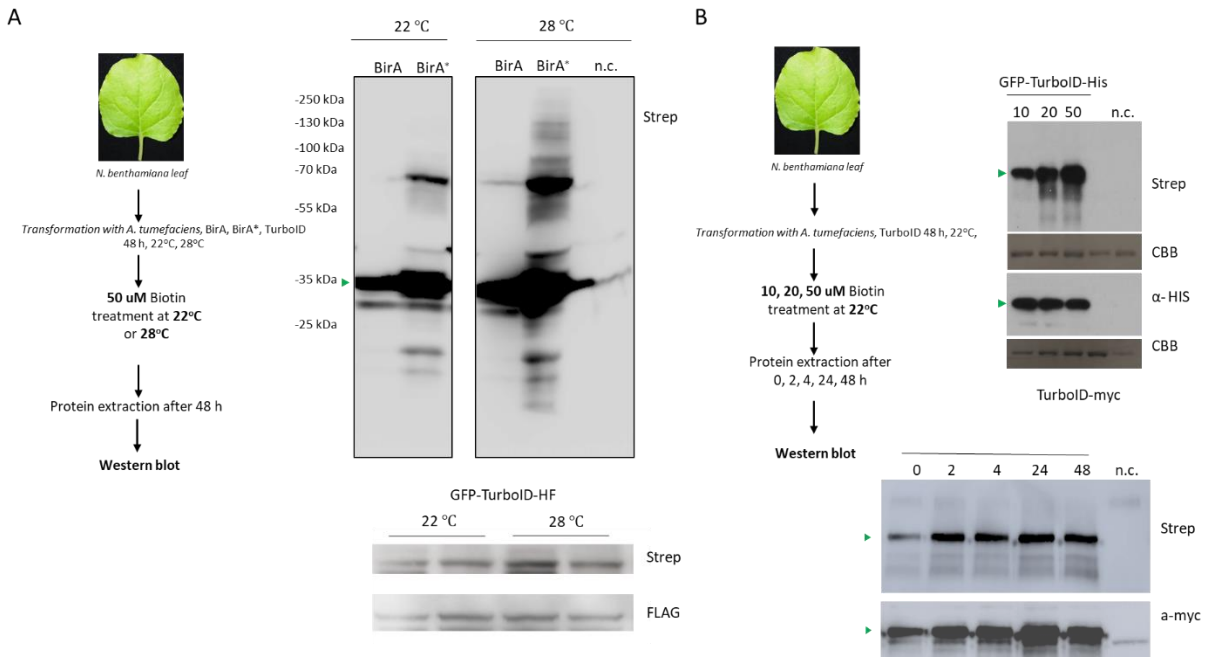

Figure S3. Biotinylation of BirA* increases at elevated growth temperature and biotin concentration in *Nicotiana benthamiana*. (A) Upper blot: The wild-type version of BirA shows residual cis-biotinylation activity at both 22°C and 28°C. BirA* (BioID) shows promiscuous biotinylation which increases with temperature. Bottom blot: GFP-TurboID-HF activity was ~2 fold increased at higer temperature (i.e. when going from 22°C to 28°C). Two biological replicates are depicted. (B) Increasing biotin levels elevated biotinylation efficiency and efficient cis-biotinylation was observed already 2 h after biotin administration. Green arrowheads show the corresponding BL. N.c. negative control.

Noteworthy, the effect of temperature on TurboID activity was less apparent compared to that of BioID, consistent with the temperature-dependency of the two enzymes [9]. Interestingly, similar to GFP-TurboID expressed in the hairy root cultures, biotinylation reaches its highest cis-biotinylation level already 2 h after biotin administration in *N.benthamiana* (**Supplemental**

Figure 3B). TurboID and mTurboID were the only PBLs in plants with biotinylation efficiency occurring in the range of few hours, as other PBLs did not show any visible sign of trans-biotinylation in that time **(Figure 1 and Supplemental Figure 2**).

TurboID can be used for the efficient capture of plasma membrane interactomes in Nicotiana benthamiana

Next, we tested whether we could achieve biotinylation of protein interactors using PDL under the conditions established for *N. benthamiana*. We observed that the prey proteins used in plants for BioID so far were relatively small proteins (i.e. HopG, 25 kDa [20], OsFD2 18 kDa [18], AvrPto 16 kDa [19]). Interestingly, all these proteins have a smaller predicted radius (assuming a globular shape) than all four PBLs used in the PDL approaches so far.

We tested our conditions for PDL using as test-cases plasma membrane-localized protein complexes with radii within a range of a few nm. First, we used a known membrane receptor complex from *Lotus japonicus* comprised of two symbiotically active receptor kinases: The LysM-type RLKs NOD FACTOR RECEPTOR 5 (NFR5) and the LRR-RLK SYMBIOTIC RECEPTOR-KINASE (SYMRK). These proteins assemble within the same complex in *L. japonicus* roots [24] as well as in *N. benthamiana* upon heterologous expression [25]. In contrast, the brassinosteroid receptor BRASSINOSTEROID INSENSITIVE 1 (BRI1) was shown not to be involved in this interaction as co-IP results failed to identify BRI1 in these experiments [25]. To further extend the set of control proteins, we additionally cloned the *A. thaliana* innate immune pattern recognition receptors FLAGELLIN SENSING 2 (FLS2) and the EF-TU RECEPTOR (EFR), both belonging to the LRR-family, as well as the LOW TEMPERATURE INDUCED PROTEIN LTI6b that is commonly used as a bona fide plasma membrane marker in plant cell biology [26].

We first co-expressed the symbiotic receptors NFR5 and SYMRK as C-terminal GFP fusion proteins with a cytosolic TurboID-GFP in *N. benthamiana*. Immunoprecipitation and Western Blot analysis revealed the successful expression and pull-down of all three proteins (**Figure 2A**). When probing for biotinylation levels, we exclusively detected self-biotinylation in case of cytosolic TurboID-GFP (**Figure 2A**). However, prolonged exposure of the blot resulted in weak detectable bands in case of NFR5-GFP and SYMRK-GFP indicating the presence of some background *trans*-biotinylation. To test whether *trans*-biotinylation of known interacting proteins can be observed, we generated an NFR5-TurboID and co-expressed it with SYMRK-GFP. Here, we not only detected a clear cis-biotinylation of NFR5-TurboID but also *trans*-biotinylation of SYMRK (**Figure 2B**). These data show that specific *trans*-biotinylation occurs within a known receptor complex.

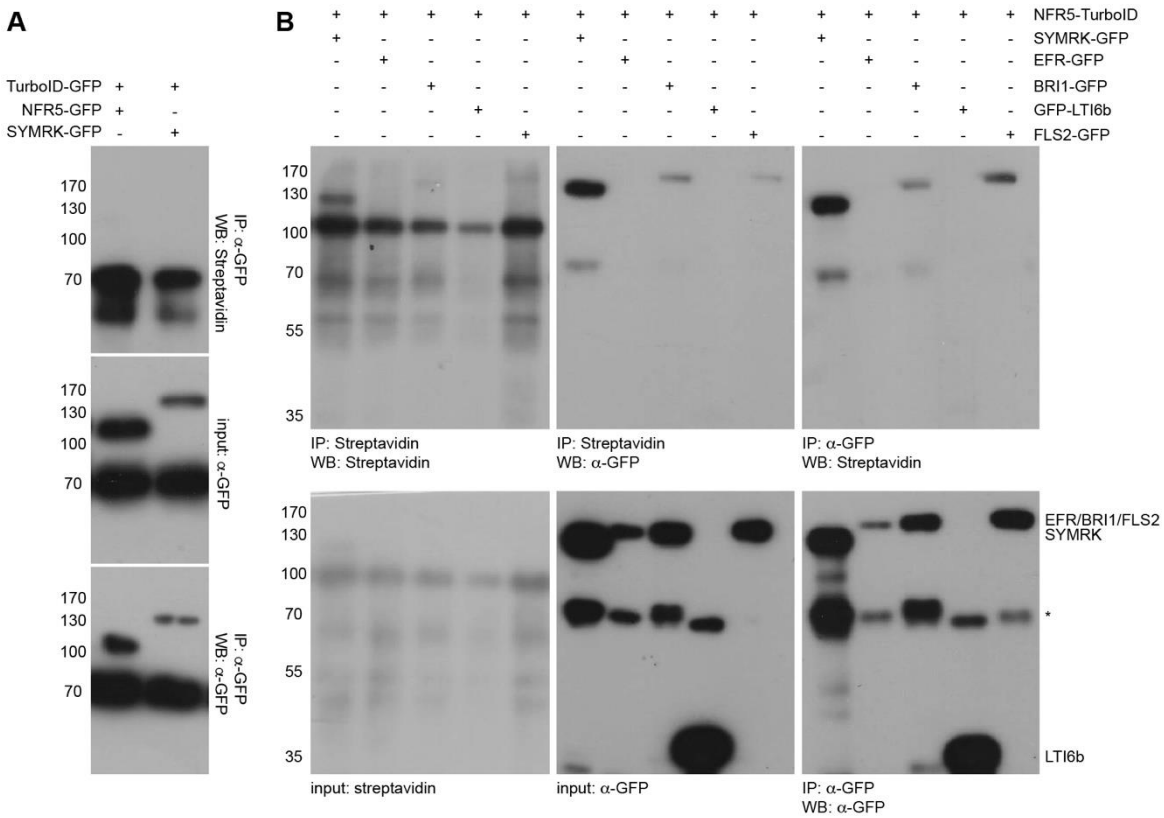

Figure 2. Trans-biotinylation within membrane-resident receptor complexes. (A) TurboID-GFP was co-expressed with symbiotic RLKs to test for unspecific *trans*-biotinylation. While all proteins were detected before (middle panel) and after immunoprecipitation (lower panel), no *trans*-biotinylation of the receptors was observed under these conditions (upper panel). The activity of TurboID is indicated by self-biotinylation of TurboID-GFP (70 kDa). (B) Fusing TurboID to NFR5 (120 kDa) resulted in strong *trans*-biotinylation of the known interaction partner SYMRK (150 kDa), weak signals were detected in case of the PM-resident receptors BRI1 and FLS2, whileno *trans*-biotinylation of EFR and the PM-marker LTI6b were detected. IP= immunoprecipitation; WB= Western Blot. *= unclassified band.

To test for specificity in the assay, we co-expressed NFR5-TurboID additionally with the functionally unrelated transmembrane RLK BRI1, which was previously shown to not interact with the NFR5/SYMRK complex using co-IP [25]. While we detected strong BRI1 expression, this protein was only weakly *trans*-biotinylated by NFR5-TurboID indicating some unspecific labelling or that the protein is in proximity to the complex (**Figure 2B**). To broaden this, we also co-expressed the transmembrane proteins FLS2, EFR and LTI6b with NFR5-TurboID. While no bands were detected for EFR and LTI6b, we observed some weak signal for FLS2 indicating that this receptor may locate in close proximity to NFR5 (**Figure 2B**). Prolonged exposure of the blots yielded some weak signal for all membrane proteins as also observed for GFP-TurboID (**data not shown**). However, these signals were orders of magnitude lower than those detected for NFR5/SYMRK. This assay was further optimized by temporally limiting the reaction. We could show that trans-biotinylation efficiently occurs within 15 min after applying exogenous biotin, demonstrating that specificity is maintained by minimizing the availability of the substrate (**Supplemental Figure 4**).

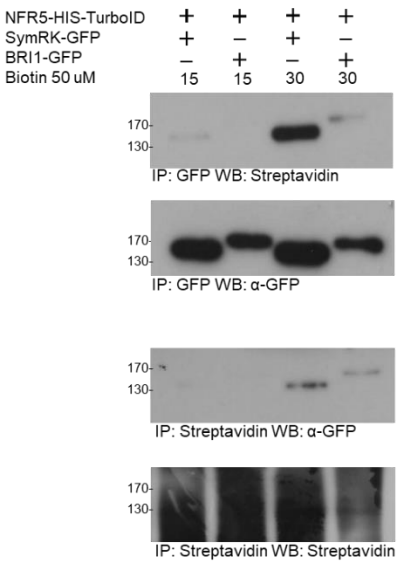

Figure S4. Temporally limiting the reaction results in weak but specifically detectable bands in case of NFR5-TurboID and SYMRK-GFP. Biotin was applied for 15 or 30 min. IP= immunoprecipitation; WB= Western Blot.

It should also be considered that in addition to ectopic expression of the constructs, the weak dimerization potential of GFP here or other protein tags with similar properties may result in potentially unspecific *trans*-biotinylation.

Taken together these data clearly show that TurboID-mediated PDL can be efficiently used for membrane proteins. It can be advantageous over other methods such as co-immunoprecipitation as it does not require any optimization of the solubilization conditions and it provides the possibility to detected transiently protein complex constituents.

Application of PDL in Arabidopsis thaliana cell cultures using the TPLATE complex as a case study

Next, we surveyed the efficiency of *trans*-biotinylation for a stable multi-subunit plant protein complex. As a test case, we took the plasma membrane-associated octameric TPLATE complex (TPC) [27] and used stably transformed *A. thaliana* culture cells as a third model system.

Given the higher biotinylation level observed in *N. benthamiana* at 28°C (**Supplemental Figure 3**) we tested different labelling conditions using *A. thaliana* suspension cell cultures. We grew the cells expressing TPLATE-BioID and GFP-BioID, i.e. proteins fused to the initial version of BirA*, at various temperatures in the presence of 50 µM biotin for 24 h. We subsequently isolated the complex using streptavidin affinity purification (see **Materials and Methods**), performed tryptic on-bead digest and analyzed the released non-biotinylated peptides using LC-MS/MS.

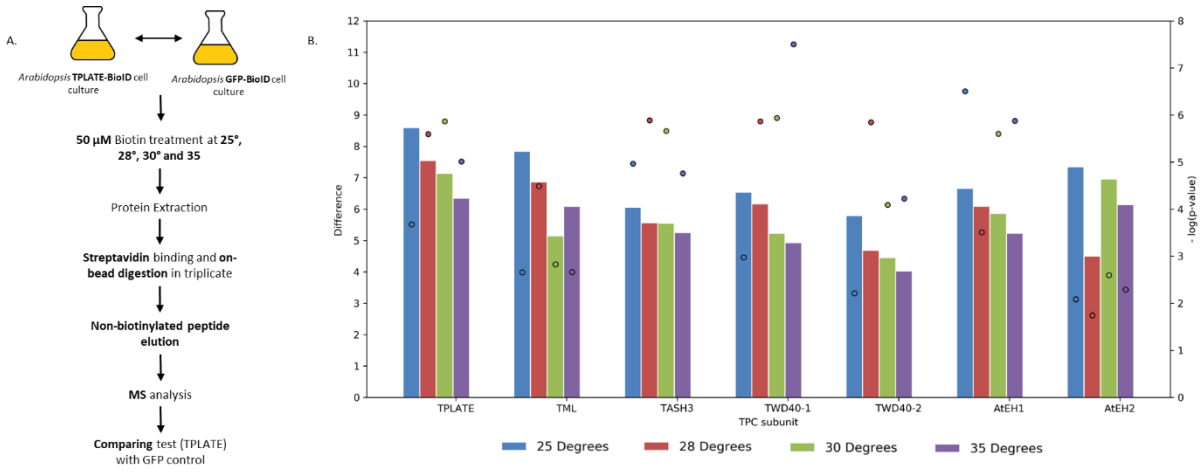

Figure 3. Detection of TPC subunits with TPLATE-BioID is optimal at 28° C. (A) Experimental setup to look for enriched TPC subunits in biotin treated transformed *Arabidopsis* cell cultures. (B) Fold change abundance of the TPC subunits and statistical significance (-log(p-value)) compared to control. Fold change and p-values were calculated from the average LFQ intensities for 3 technical replicates of TPLATE-BioID w.r.t.versus GFP-BioID at similar temperature. Cell cultures were incubated with 50µM biotin at 25°-35°C for 24 h before harvesting. The TPC subunits are detected at all 4 temperatures without major differences. At 28°C and 30°C, the overall detection of several of the other subunits shows increased robustness (p-value) compared to both the lower (25°C) and higher (35°C) temperatures.

In order to compare the effect of temperature on the biotinylation efficiency to identification of proteins from isolated protein complexes, we focused on the other seven TPLATE complex members and compared their abundance and fold changes after streptavidin-purification as deduced from label-free protein quantification (LFQ; [28]) to the control setup (35S::GFP-BioID) (**Figure 3A**). The fold change difference with respect to the control for the

other TPC subunits was subunit dependent and not dramatically different between the different temperatures. The highest overall fold change difference for the different subunits, combined with the optimal robustness of the identification (p-value) was detected at 28°C (**Figure 3B, Supplemental Data Set 1**), indicating that this temperature presents the optimal trade-off between biotinylation efficiency of BioID and perturbation of physiological processes due to elevated temperatures.

Various PBLs affect biotinylation of TPC subunits differently

The introduction of a flexible linker has been successfully used to extend the labelling radius of PBLs [8], which is estimated to be about 10 to 15 nm [10]. This increased labelling radius may be desirable when the protein of interest is significantly larger than the labelling radius of the PBL alone, and/or when the goal is to map the constituency of a larger protein complex or discrete subcellular region. We thus compared the efficiencies of various PBLs and assessed their biotinylation radius by inserting a long flexible linker. For this, *Arabidopsis* cultures expressing C-terminal fusions of TPLATE with BioID or BioID2 were assessed, with and without a 65 aa linker similar to the one that was reported before [5]. As controls, we generated GFP fused to BioID or BioID2 without additional linker **(Supplemental Figure 5)**.

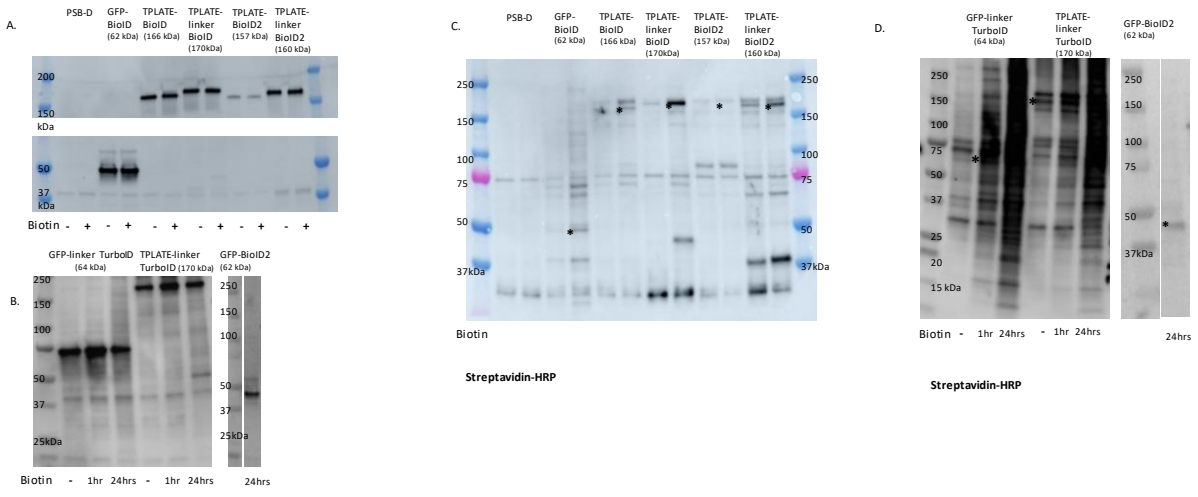

Figure S5. Different PBL cause different self- and trans- biotinylation. Cell cultures expressing different TPLATE-PBL were incubated with 50µM biotin at 28°C for 1 h and 24 h before harvesting. (A and B) Anti-HA HRP western blotting was performed to visualize expression levels of the different cultures. (C and D) Streptavidin-HRP western blotting of different TPLATE-PBLs, GFP-BioID and control cell cultures (PSB-D). Self-biotinylation of the bait and *trans*-biotinylation can .clearly be observed. * indicates self-biotinylation of the bait.

Next, we tested the activity of different PBLs in this system. We grew the cultures for 24h at 28ºC, with and without exogenous biotin, and assessed expression and biotinylation via Western blotting (**Supplemental Figure 5**). Protein abundance of the BioID and BioID2 constructs was comparable to their respective controls in our cell cultures and not affected by the addition of biotin. Only the levels of TPLATE-BioID2 were somewhat lower. At the level of cis- and *trans*-biotinylation, we observed different patterns for each of the enzymes used. As several of the detected bands which increased significantly in the presence of biotin, did not correspond to bands in the control (PSB-D) or GFP-BioID culture, they likely represent different *trans*-biotinylated interactors and suggest that the outcome of a BioID-based interaction assay might (partially) depend on the PBL used. TPLATE-linker PBL showed the most diverse biotinylation pattern when comparing to the other setups expressing BioID and BioID2 fusions (**Supplemental Figure 5**) suggesting that adding a linker may be used to to optimize proximity labelling. Consistent with the results described for tobacco, linkerTurboID constructs showed some biotinylation without the addition of exogenous biotin, increased biotinylation after 1 h incubation with biotin and extensive biotinylation after 24 h incubation with biotin in both control and bait cultures suggesting it is highly promiscuous.

As observed in *N. benthamiana* (**Supplemental Figure 2**), BioID outperformed BioID2 using TPLATE as bait in this system, although this might be skewed due to lower expression levels of the latter. Adding a flexible linker increased self-biotinylation levels of the bait compared to the constructs without linker (**Supplemental Figure 5A and C**). Our results are consistent with previous observations in non-plant systems suggesting that linkers increase the biotinylation output [8].

Following the positive effect of exogenous biotin supplementation (**Supplemental Figures 2 and 3**), we tested the effect of increasing biotin concentrations on cis-biotinylation efficiency. Cell cultures expressing TPLATE-linkerBioID were grown at 28ºC in the presence of increasing concentrations of biotin (50 µM to 4 mM) and processed for Western blotting. Supplementing the culture with concentrations of biotin in the range of 50 uM to 1 mM increased cis-biotinylation output up to a maximum of ~2-fold (Supplemental Figure 6). Increasing biotin concentration >2mM did not further increase the cis-biotinylation efficiency.

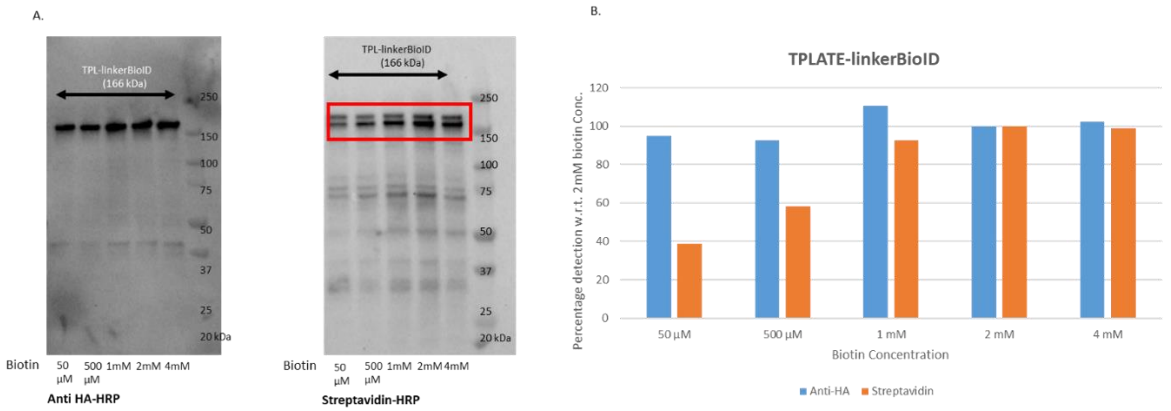

Figure S6. Cis-biotinylation of TPLATE-linkerBioID increases at higher concentration of exogenous biotin. Cell cultures expressing TPLATE-linkerBioID were incubated with biotin (50µM to 4mM) at 28°C for 24 h. (A) Anti-HA HRP western immunostaining was performed to check protein expression while streptavidin-HRP western immunostaining was used to assess the biotinylation levels of TPLATE-BioID. (B) Quantification of the percentage of biotinylation (orange) as well as the expression (blue) for each biotin concentration compared to the maximum biotinylation efficiency (2mM) using ImageJ.

We took advantage of the increased biotinylation observed by including a long linker sequence and generated *Arabidopsis* cultures expressing GFP-linkerTurboID and TPLATE-linkerTurboID. Similar to other systems, 24 h post-biotin addition, TurboID efficiency strongly outperformed all other PBLs tested as evident from the high biotinylation levels observed with and without the addition of exogenous biotin and for both the control (GFP) as well as the TPLATE expressing cultures (**Supplemental Figure 5B and D**).

In order to compare the different PBL modules, we processed the cell cultures for LC-MS/MS and focused on the relative levels of the various TPC subunits compared to the control setup. Our first mass spec results following streptavidin pull down and on-bead digestion identified all known subunits of the TPC. Given that this is a robust multi-subunit complex [27] and that we identify only non-biotinylated peptides with our on-bead digestion protocol, we assumed that the subunits we detect are a combination of direct biotinylation as well as co-immunoprecipitation of the complex as a whole. To test this, we adapted our protocol (**Figure 4A**) and included protein extraction and stringent washing steps with a buffer containing 8M urea and 2% SDS to unfold proteins captured by the beads and to be able to remove unspecific protein binders. We also included the TPLATE-linkerBioID setup treated with 2 mM biotin for 24 h to assess if increased biotin concentration improves TPC subunit detection.

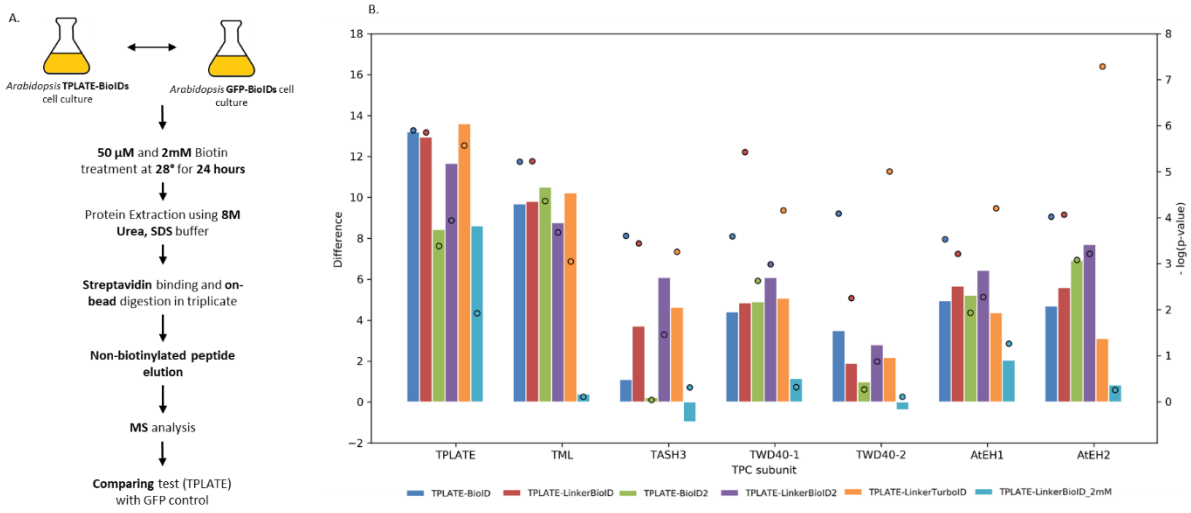

Figure 4. Different TPLATE-PBLs affect biotinylation of TPC subunits differently. (A) Experimental setup. (B) Comparison of the relative fold change and statistical significance (-log(p-value)) compared to control samples for the various PBLs and conditions. Relative fold change and p-values were calculated from the average LFQ intensities of 3 technical replicates of the test compared to the control. GFP-BioID served as a control for TPLATE-BioID and TPLATE-linkerBioID while GFP-BioID2 is a control for TPLATE-BioID2 and TPLATE-linkerBioID2 and GFP-linkerTurboID is the control for TPLATE-linkerTurboID.

In agreement with the higher stringency of the isolation procedure, the smallest TPC subunit, LOLITA, which could be robustly detected using AP-MS [27] and could be detected without being denatured prior to binding to streptavidin beads, was no longer detected (**Figure 4, Supplemental Data Set 2**). LFQ revealed that the remaining seven TPC subunits, including the bait TPLATE, could be detected using BioID, linkerBioID, linkerBioID2 and linkerTurboID. The TASH3 and TWD40-2 subunits could however hardly be detected using BioID2, which might be caused by the reduced expression level of the bait observed in these cultures (**Supplemental Figure 5**). Increasing the concentration of biotin to 2mM had an adverse effect on the detection of the TPC subunits as only the bait itself could be identified. It is likely that increasing biotin concentrations causes residual free biotin to accumulate in the protein extract, even after protein desalting to deplete free biotin, thereby occupying the streptavidin binding sites on the beads (saturated at >9 µM of biotin). We tested this "saturation hypothesis" using *N. benthamiana* leaves and protein precipitation to completely remove residual biotin, showing that even low concentration of residual biotin can saturate the streptavidin beads and incapacitate detection (**Supplemental Figure 7**). Hence, special care should be taken to avoid excess of residual free biotin during streptavidin-capture.

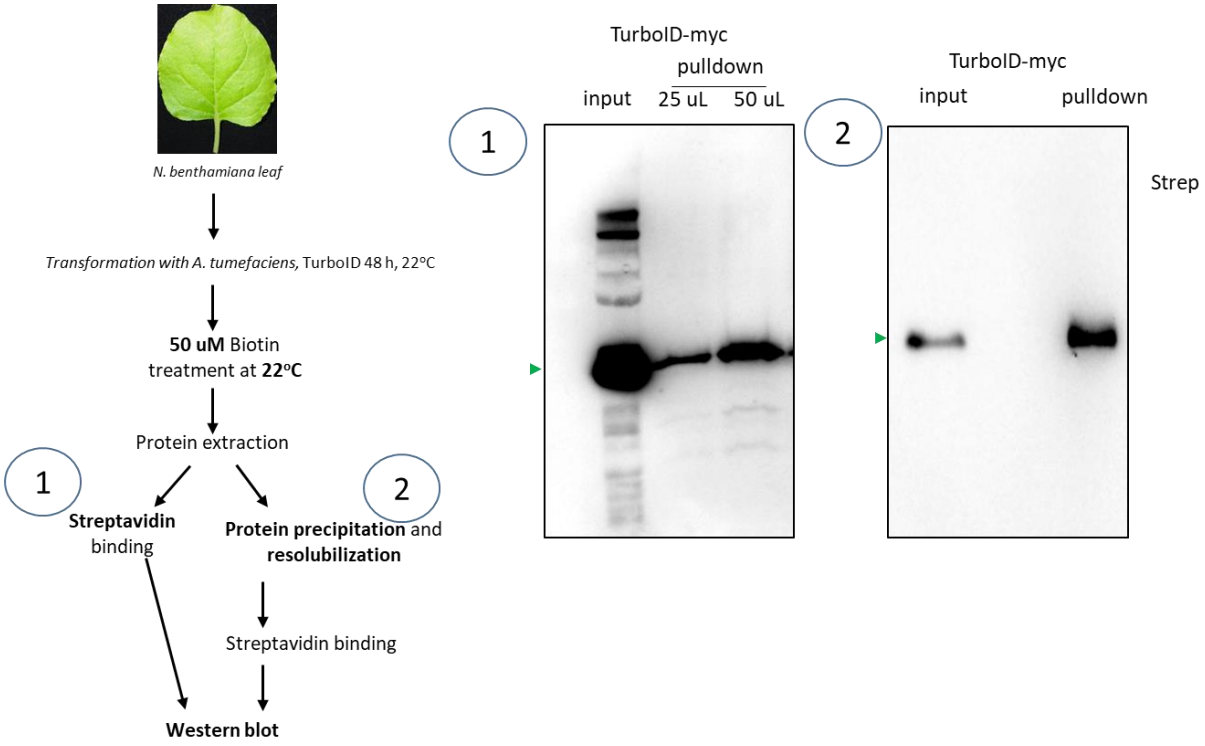

335

Figure S7. Exogenous application of biotin can exceed the binding capacity of streptavidin beads. Blot on the left: input and IP with streptavidin using 25 or 50 ul of beads. Note that 2 x more beads increased the recovery of the input signal, suggesting that the beads are saturated. Blot on the right: IP with 25 ul of streptavidin beads but in this case the supernatant was precipitated using ammonium acetate to remove excess biotin. Green arrowheads mark the position of the BL.

336

337 It should be noticed that the fold change by which the other TPC subunits were detected with
338 TurboID was only similar or even sometimes lower (e.g. AtEH2) compared to the other BioID
339 forms (Figure 4). This was caused by the fact that TPC subunits were identified more in the
340 TurboID control samples, resulting in the lower relative fold changes. All individual TPC
341 subunits were detected with more than 20 unique peptides using the GFP-linkerTurboID
342 whereas TWD40-2 was the only TPC subunit detected in other GFP-PBLs, which explains its
343 overall low fold change (**Supplemental Table 3**). Nevertheless, TurboID identified the other
344 TPC subunits more robustly compared to the other PBLs. So, although in our case, TurboID
345 showed to be superior to all others in identifying the other TPC subunits, the lower signal/noise
346 ratio of TurboID, due to its increased activity, might work as a disadvantage to observe
347 differences between bait proteins and control samples, which might even be enhanced if the
348 proteins are targeted to specific subcellular locations.

349

Supplemental Table 3: Cell cultures expressing different TPLATE-PBLs identifies TPC subunits with different amount of non-biotinylated peptides. The table shows the amount of non-biotinylated peptides identified for TPC subunits in GFP and TPLATE-BioIDs PBL cell cultures. Preparation of samples for LC-MS/MS involved the use of a buffer containing 8M Urea and 2% SDS. Cell cultures were incubated with either 50µM or 2mM biotin for 24 hours before harvesting. This table shows higher amount of peptides detected for all TPC subunits in case of linkerTurboID constructs than other BioIDsPBL. Also, it show higher amounts of peptides detected in TurboID control experiments (GFP-linkerTurboID vs. GFP-BioID and GFP-BioID2) suggesting increased promiscuity of TurboID.

Total number of non-biotinylated peptides identified for each TPC subunit							
	AT1G20760.	AT1G21630.	AT2G07360.	AT3G01780.	AT3G50590.	AT5G24710.	AT5G57460.1
	AtEH1	AtEH2	TASH3	TPLATE	TWD40-1	TWD40-2	TML
SUM TPLATE linkerTurboID	76	158	205	384	228	374	116
SUM GFPlinkerTurboID	40	98	122	27	102	271	21
SUM TPLATE BioID	20	32	2	428	68	95	37
SUM TPLATE linkerBioID	19	37	15	540	35	34	16
SUM GFP BioID	-	-	-	-	-	26	-
SUM TPLATE BioID2	9	30	-	157	42	38	51
SUM TPLATE linkerBioID2	24	55	59	453	107	89	38
SUM GFP BioID2	-	-	6	-	-	42	-
SUM TPLATE linkerBioID 2mM	-	-	-	10	-	-	-

The structural compostion of protein complexes causes differences in detection between PDL and APMS

We compared the stoichiometry by which the different TPC subunits are detected using PDL using our stringent washing protocol with our one step IgG pull down protocol using the GS^{rhino} TAP tag. To do this, we normalized the LFQ intensities for each TPC subunit to TPLATE and compared the values of TPLATE-linkerBioID, TPLATE-linkerBioID2 and TPLATE-linkerTurboID with those coming from tandem affinity tag (TAP)-fused TPLATE (TPLATE-GS^{rhino}). Compared to the bait protein (TPLATE), the other TPC subunits are detected with small differences in relative abundance between the different subunits in one-step-purification MS as well as with PDL which showed the same trend. (**Figure 5, Supplemental Data Set 3**). Our results, comparing BioID, BioID2 and TurboID, each fused to TPLATE and having a long linker in-between reveal that TurboID allows identifying the other subunits with higher enrichment compared to the other PBLs. The smallest subunit, LOLITA, could only be identified via TAP-MS, which points out that this subunit is not biotinylated although it harbours 11 lysine residues. Our results furthermore reveal that, except for LOLITA, all TPC subunits, which are part of a protein complex in the range of 1MDa can be identified using our stringent wash protocol as proxy for biotinylation. For example, using TPLATE as bait and using a long linker sequence linking it to the PBL, the TASH3 subunit was detected with 15 peptides instead of 2 in the absence of the linker (**Supplemental Table 3**).

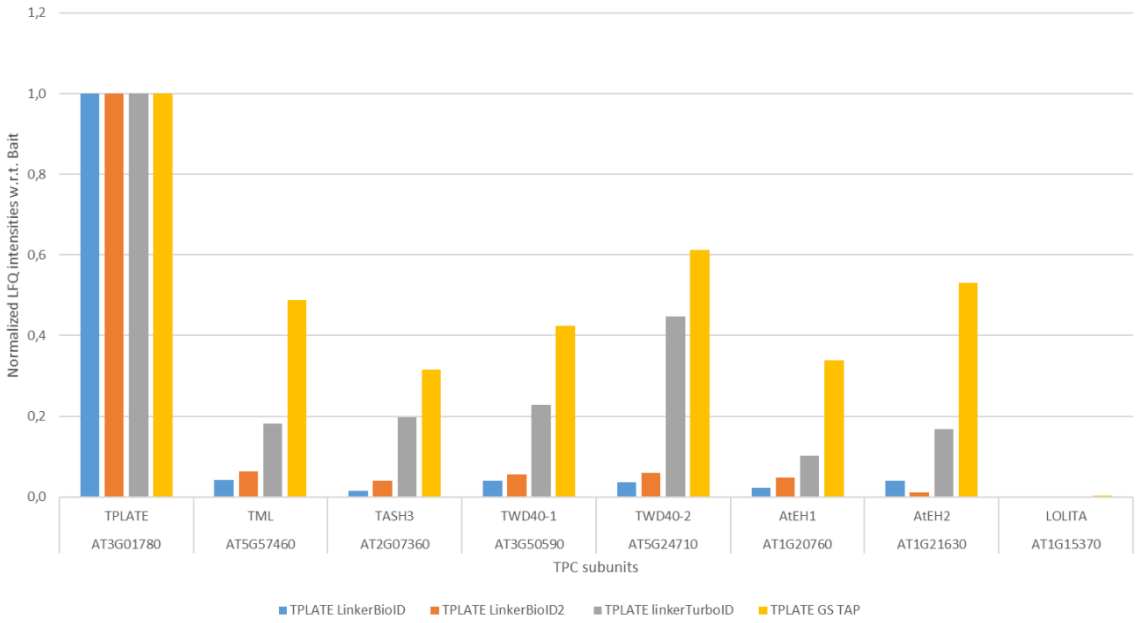

Figure 5. Comparison of relative abundance of TPC subunits in pull down and BioID. Pull down and LinkerBioIDs experiments were performed in triplicate, using TPLATE as bait. Per set of experiments, average LFQ intensities were calculated for each of the TPC subunits. Values were normalized versus the bait, TPLATE, taking into account the molecular weight of the TPC subunit. Normalized LFQ values show small differences in relative abundance of the TPC subunits, both in pull down and BioID.

371

372 ***Identification of biotinylated peptides allows identifying structural relationships between***
373 ***complex subunits***

374 The interaction between biotin-streptavidin is strong enough to be retained even under harsh
375 conditions, e.g, in reductive buffers (**Supplemental Figure 7**). Thus, biotinylated peptides are
376 expected to be retained on the streptavidin beads even under stringent washing. Following
377 stringent washing under denaturing conditions, on bead digest will release non-biotinylated
378 proteins, which can subsequently be identified using LC-MS. This approach, however, does
379 not provide direct evidence for biotinylation and it relies on the assumption that only
380 biotinylated proteins remain bound to the beads after the washing steps. To acquire direct proof
381 of biotinylation MS-based identification of biotinylated peptides is required.

382

383

384

385

386

387

388

389

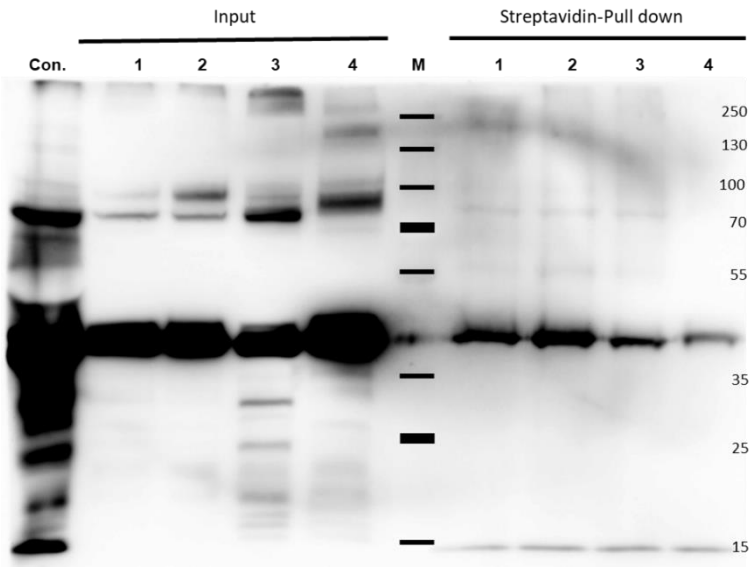

Figure S8. The biotin-streptavidin interaction is retained under harsh conditions. Different extraction buffers were used for testing the binding affinity of biotin-labelled proteins with streptavidin from equal amount of plant protein material: 1. 50mM HEPES, 150 mM NaCl, 0.5% NP40, 10% Glycerol, 1mM PMSF; 2. 50mM Tris/HCl, 150 mM NaCl, 0.5% NP40, 10% Glycerol, 1mM PMSF; 3. 1x PBST, 1mM PMSF; 4. 2x Laemmli sample buffer (65 mM Tris-HCl, pH 6.8, 20% (w/v) glycerol, 2% SDS, 0.01% bromophenol blue, 10mM DTT). Con: control. M: marker. Note that the lack of enrichment in the pulldown (right panel) is due to the presence of biotin (see also **Supplemental Figure 7**).

Thus, we expanded the protocol to also be able to identify biotinylated peptides. For this, we included a second elution step (see **Materials and Methods**) to release the biotinylated peptides from the beads using an adapted protocol based on [29]. This approach allows detecting both non-biotinylated as well as biotinylated peptides in the same experimental setup. We performed the analysis on the TPLATE-linkerTurboID setup and again specifically focused on peptide identification of the TPC subunits (**Figure 6** and **Supplemental Data Set 4**). The highest number of biotinylated peptides were identified for TPLATE (44 biotinylated peptides), followed by TWD40-1 (18), EH2 (16), EH1 (12), TWD40-2 (9) and TML (3). No biotinylated peptides could be detected for LOLITA, correlating with our previous results. Mapping non-biotinylated and biotinylated peptides, taking into account their relative abundance, on the different TPC subunits revealed differences in the number of detected peptides as well as differences in the distribution of the biotinylated peptides along the length of the subunits. Whereas the bait, TPLATE, shows a relatively even distribution of biotinylated peptides along the protein sequence, there is a clear tendency of the EH1, EH2 and TML subunits towards biotinylation at their C-terminal parts **(Figure 6)**. It is tempting to speculate that the observed distribution of biotinylated peptides, as well as their absence, reflect the proximity of the domains as well as structural constraints with respect to the bait protein and

409 that proximity biotinylation harnesses the potential to help deduce structural insight into protein
410 complexes as well as topology information in case of transmembrane proteins.

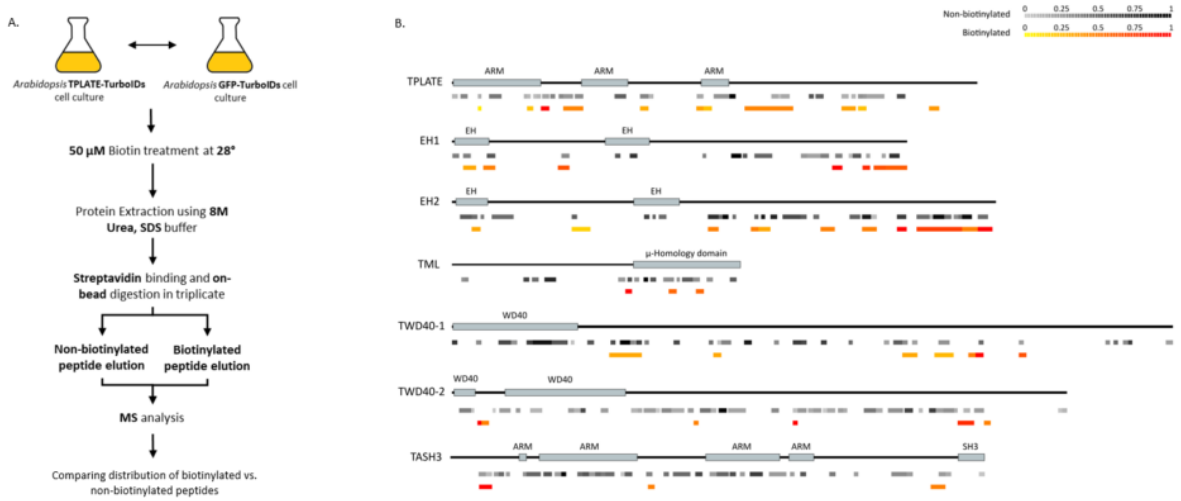

411

Figure 6. Comparison of biotinylated versus non-biotinylated peptide identification of the various TPC subunits using TPLATE-linkerTurboID as bait. (A) Experimental setup. (B) Overview of the identified peptides and their abundance, mapped onto the different TPC subunits.

412

413 ***Discussion***

414 We provide a comprehensive comparison of various PBL based proximity labelling strategies
415 in plants and show that TurboID is the most promiscuous one, and that this also sometimes
416 leads to a lower signal to noise ratio. We also provide guidelines and approaches for
417 interactome capture in various plant systems specifically focusing on the ones that interact with
418 the plasma membrane. Furthermore, we show that for each bait/system conditions need to be
419 optimized independently.

420 We observed that in all three plant systems, using exogenous application of biotin
421 enhances PDL output but might not be a strict requirement for the successful application of
422 PDL. This result seems to contradict with what has been reported for a related method called
423 INTACT (isolation of nuclei tagged in specific cell types) in plants. This method allows for
424 affinity-based isolation of nuclei from individual cell types of tissue. INTACT relies on the
425 endogenous pool of biotin as no exogenous supplementation is required [30]. In INTACT,
426 nuclei are affinity-labelled through transgenic expression of the wild-type variant of BirA
427 which biotinylates a nuclear envelope protein carrying biotin ligase recognition peptide from
428 ACC1. This tag acts as a native substrate for the *E. coli* biotin ligase BirA [31]. The use of
429 wild-type BirA along with its preferable substrate could explain the higher affinity for the free
430 biotin pool in INTACT, and the peptide used as fusion is an optimal substrate for the bioAMP

intermediate. We assume that various proteins may show variability in functioning as acceptors of bioAMP (e.g. depending on the presence of accessible lysine residues).

PDL utilizing bacterial enzymes poses the question of whether these enzymes could perform adequately in plants [8]. The activity optimum for BioID2 is 50ºC, whereas for BioID this is 37ºC and thus BioID2 may be most adequate for use at higher temperature conditions. Both temperatures are however far-off from the usual growth temperatures of most plant species grown in temperate regions (e.g. Arabidopsis sp.). Both BioID2 and BioID show reduced activity below 37ºC ([8] and our results herein). Furthermore, the lower temperature optimum of TurboID (and mTurboID) [9] would imply that may function better at normal plant growth temperature. In fact, we observed that TurboID activity is only increased by 2-fold from 22ºC to 28ºC. We, however, cannot rule out that the optimal temperature for PDL may vary depending on the bait protein. At all tested temperatures, we observed that TurboID (and mTurboID) outperforms other PBLs in terms of speed and promiscuity. Hence, TurboID might be preferable when it comes to initial study of (transient) complex composition where the generation of as much as possible specific biotinylation output in short time might be desirable.

However, the strong promiscuity of the control might also work as a disadvantage in revealing specific interactions in cases where the reaction cannot be controlled that easily in time or when both the bait and the control would be targeted to a confined intracellular space.

We provide evidence that our methods and conditions are applicable to plasma-membrane complexes. We showed that the interaction of the symbiotic RLKs NFR5 and SYMRK can be identified by exploiting PDL and particularly the PBL TurboID. Furthermore, the use of proper negative controls is imperative. However, even though the brassinosteroid receptor BRI1 was not co-immunoprecipitated with the symbiotic receptors in a previously published dataset [25], we detected weak biotinylation of this RLK and the immune-receptor FLS2. While it could be interpreted as unspecificity within the PBL system, it should also be considered, that PBL allows labelling of transient interactions or proximal proteins. As a consequence, continuous unstable interactions accumulate to detectable amounts of proteins and would thus allow their identification. As PDL using TurboID is capable of *trans*-biotinylation in the range of minutes (15 minutes under our experimental conditions), the enrichment of unstable interactions would thus be more prominent. Therefore, putative interactions identified by PBL still need to be verified using independent experimental systems but comparisons between the different experimental systems should always reflect the technical limitations of each approach.

By expanding our protocols and PBLs into Arabidopsis cell cultures, we could reproduce the composition of the TPC except for one subunit. We show that the use of linkers can be advantageous when it comes to identifying protein-protein interactions of multi-subunit complexes. Furthermore, TPLATE-linkerBioID2 shows reduced cis-biotinylation compared to TPLATE-linkerBioID in the presence of exogenous biotin but seems to function in the absence of biotin suggesting that in plants, BioID2 can function in tissues where exogenous supplementation of biotin may be slower, e.g. the vasculature. Furthermore, increased biotin applications can lead to serious impediments when it comes to the identification of TPC subunits as this can interfere with biotinylated protein binding on streptavidin slurries. Caution is warrented to assure sufficient capture capacity of biotinylated proteins', since the amount of beads needed for capture should be tested for each experimental setup/protocol.

Finally, by establishing a strategy for simultaneous identification of biotinylated and non-biotinylated peptides we could provide evidence for the accessibility of different protein parts to PDL. We show that EH1, EH2 and TML subunits are preferentially biotinylated at their C-terminal parts, suggesting that their C-termini are in closer proximity to the C-terminal end of TPLATE and/or some domains (even complex subunits) are not available for biotinylation. We thus provide evidence that PDL approaches in plants may be able to provide structural information of multi-subunit protein complexes and that this may be extended to the topology of membrane proteins.

While this manuscript was on preparation, two additional works appeared in BioRxiv making use of TurboID in plants. These two works complement our work providing further evidence that TurboID can be used to capture cell-specific interactomes [32] and transient signalling components [33]. Taken together, these three studies provide a new arena for the identification of novel protein-protein interactions in plants.

Supplemental Table 1: list of constructs used

Name	Vector	Promoter	Gene	PBL used
GFP-BioID	pK7m34Gw	p35s	GFP	BioID
GFP-BioID2	pK7m34Gw	p35s	GFP	BioID2
TPLATE-BioID	pK7m34Gw	p35s	TPLATE	BioID
TPLATE-BioID2	pH7m34Gw-R	p35s	TPLATE	BioID2
TPLATE-linkerBioID	pH7m34Gw-R	p35s	TPLATE	$(GGGGS)_{13}$ BioID
TPLATE-linkerBioID2	pH7m34Gw-R	p35s	TPLATE	$(GGGGS)_{13}$ BioID
GFP linkerTurboID	pK7m34Gw	p35s	GFP	$(GGGGS)_{13}$ TurboID
attL2-BioID-attL3	pG9m-2	-	-	bioID

attL2-BioID2-attL3	pG9m-2	-	-	bioID2
attL2-linkerBioID-attL3	pUC54	-	-	(GGGGS)13 BioID
attL2-linkerBioID2-attL3	pG9m-2	-	-	(GGGGS)13 BioID2
attL2-linkerTurboID-attL3	pUC54	-	-	(GGGGS)13 TurboID
TPLATE-linkerTurboID	pK7m34Gw	p35s	TPLATE	$(GGGGS)_{13}$ TurboID
BirA-myc	pICSL86900	p35s	BirA-myc	BirA-myc
BirA*-myc	pICSL86900	p35s	BirA*-myc	BioID-myc
HF-BioID2-HA	pICSL86900	p35s	BioID2-HA	BioID2-HA
GFP-TurboID-HF	pICSL86922	p35s	TurboID-HF	TurboID
GFP-TurboID-His	Xpre2-S (pCAMBIA)	P35S	GFP	TurboID
NFR5-TurboID	Xpre2-S (pCAMBIA)	P35S	NFR5	TurboID

Supplemental Table 2: list of primers used

Name	Primer
BirA	GTGGTCTC A T TCG GGA AAC GCGGCT ATT AGA TCA AAG GAT AAC ACC GTG CCA CTT A
BirA	GTGGTCTC A AAGC CTA CAG ATC CTC TTC TGA GAT GAG TTT TTG TTC TTT TTC TGC ACT ACG AAG G
BirA	GTGGTCTC A CGTAGAGGTCGTAAATGGTTTTC
BirA	GTGGTCTC C TACGTCCACGACCAGCCTGCT
HF-Module-Fw	GTGGTCTC ACCATGGGTTCCGGAAGAGGATCGCA
HF-Module-Rv	GTGGTCTC ACATTCCCTTGTCATCGTCATCCTTG
BioID2 with long-linker-Module-Fw	agGAAGACaaTTCGGGATCTGGAGGTGGCGGAAG
BioID2 without linker-Module-Fw	agGAAGACaaTTCGTTTAAGAACTTGATATGGCTGAAAG
ScFv-superfolder-GFP-Module-Fw	GTGGTCTC A ATGG GCCCCGACATCGT
ScFv-superfolder-GFP-Module-Fw	GTGGTCTC A CGAA CCACCTTTGTAGAGCTC

MATERIAL AND METHODS

Bacterial strains

For cloning, *Escherichia coli* strain DH10B or Top10 was used using standard chemical transformation protocols. Electrocompetent *Agrobacterium tumefaciens* C58C1 Rif^R (pMP90), AGL1 Rif^R or GV3101 Rif^R bacterial cells (i.e. a cured nopaline strain commonly used for tobacco infiltration [34] were used for electroporation and tobacco infiltration. Electrocompetent rhizogenic *Agrobacterium* (RAB) ATCC15834 (ATCC® 15834™)[35] bacterial cells were used for electroporation and for hairy root transformation.

Electrocompetent *Agrobacterium tumefaciens* C58C1 Rif^R (pMP90) or GV3101 Rif^R bacterial cells (i.e. a cured nopaline strain commonly used for tobacco infiltration [34] were used for *Arabidopsis* cell culture transformation. For cloning, *Escherichia coli* strain DH10B was used using standard chemical transformation protocols. Electrocompetent *Agrobacterium tumefaciens* C58C1 Rif^R (pMP90) or GV3101 Rif^R bacterial cells (i.e. a cured nopaline strain commonly used for tobacco infiltration [34] were used for *Arabidopsis* cell culture transformation.

Cloning of the proximity label-tagged control constructs

For constructs used in hairy roots: Constructs encoding the full-length ORF of the PBL (e.g. BirA* (pDEST-pcDNA5-BirA*-Flag C-term, a kind gift from the Gingras laboratory (Couzens, Knight et al. 2013)), BioID2 (MCS-BioID2-HA, Addgene, Plasmid #74224 (Kim, Jensen et al. 2016)), TurboID (V5-TurboID-NES_pCDNA3, Addgene, Plasmid #107169 (Branon, Bosch et al. 2018)), miniTurboID (V5-miniTurbo-NES_pCDNA3, Addgene, Plasmid #107170 [9] and Apex2 (linear DNA sequence synthesis) were PCR amplified using Q5® High-Fidelity DNA Polymerase (New England Biolabs, Cat n° M0491) with oligonucleotide primers containing attB recombination sequences. The forward and reverse primer additionally encoded the GGGGS linker and the Flag-tag (DYKDDDDK) followed by a stop codon, respectively. The primer sequences are depicted in **Table S2**. The resultant attB-flanked PCR products were used in a Gateway® BP recombination reaction with the pDONR™ P2r-P3 vector (Life Technologies, Carlsbad, CA, USA) according to the manufacturer's instructions, thereby creating an entry clone. The construct was transformed in DH5α chemical competent cells and verified by sequencing (i.e. Sanger sequencing). Using a standard multisite (3-fragment) Gateway® LR cloning strategy as described by [36], the entry clones together with pEN-L1-F-L2 encoding eGFP [37] (https://gateway.psb.ugent.be/search) and pEN-L4-2-R1 encoding the constitutive cauliflower mosaic virus (CaMV) 35S promoter [37], were recombined with the multisite Gateway destination vector pKm43GW [37] to generate expression constructs. More specifically, the multisite LR Gateway reaction resulted in translational fusions between the eGFP and the proximity labels, driven by the 35S promoter. This way, the following expression constructs were created; Pro35S::eGFP-BirA*, Pro35S::eGFP-BioID2, Pro35S::eGFP-TurboID and Pro35S::eGFP-miniTurboID and Pro35S::eGFP-BirA*(Deep) construct (in pKm43GW), with a C-terminally triple HA-tagged BirA* fused to eGFP.

For constructs used in *N. benthamiana*: original BioID, BioID2 and TurboID DNA sequences were taken from [5, 9, 10], codon optimized to *Arabidopsis*. The GOLDENGATE compatible BirA, BirA*, BioID2 and TurboID were synthesized and codon optimized using the codon optimization tool of Integrated DNA Technologies, Inc. The ORFs were synthesized with BsaI overhands and were ligated to the Level1/2 vector pICSL86900 and pICSL86922, as previously described [38]. The following expression vectors were used: Pro35S::BirA-Myc, Pro35S::BirA*-myc, Pro35S::HF-BioID2-HA and Pro35S::superfolderGFP-TurboID-FLAG.

The genomic sequence of NFR5 and the coding sequence of BRI1 was synthesized with BsaI overhangs for Golden Gate as Level1 vector [39]. Pro35S::NFR5-TurboID and Pro35S::BRI1-GFP were created by Golden Gate cloning in Xpre2-S (pCAMBIA) vectors (Binder et al 2014). Pro35S::FLS2-GFP was kindly provided by Hemsley lab, University of Dundee, Scotland. Pro35S::EFR-GFP [40] and Pro35S::SymRK-GFP/ Pro35S::NFR5-GFP [41, 42] were kindly provided by Cyril Zipfel (University of Zurich, Switzerland) and Jens Stougaard (Aarhus University, Denmark).

For constructs used in *A. thaliana*: BioID and BioID2 DNA sequences were taken from [5, 10], codon optimized to *Arabidopsis* using the codon optimization tool of Integrated DNA Technologies, Inc. The BioID and BioID2 with and without linker $(GGGGS)_{13}$ with stop codon, flanked by attB2 and attB3 sites [43] were synthesized by Gen9. The TurboID sequence (Tess et al., 2018) was codon optimized to *Arabidopsis* using the codon optimization tool of Integrated DNA Technologies, Inc. TurboID with linker $(GGGGS)_{13}$ with stop codons, flanked by attB2 and attB3 sites [43], was synthesized by GenScript. Entry clones of eGFP [44], TML (At5g57460) [27] and TPLATE (At3g01780) [45] without stop codon were used in a triple Gateway LR reaction, combining pK7m34GW or pH7m34GW [43], pDONRP4-P1R-35sp and pDONRP2-P3R-BioID/BioID2/$(GGGGS)_{13}$ BioID/$(GGGGS)_{13}$ BioID2/$(GGGGS)_{13}$ TurboID to yield pK7m34GW,35sp: GFP/TPLATE/TML-BioID, pK7m34GW,35sp:: GFP/ TML-BioID2, pH7m34GW,35sp:: TPLATE-BioID2, pK7m34GW 35sp:: TML-$(GGGGS)_{13}$ BioID/BioID2, pK7m34GW 35sp:: TPLATE-$(GGGGS)_{13}$ BioID/BioID2 and pK7m34GW 35sp:: GFP/TPLATE-$(GGGGS)_{13}$ TurboID.

Plant transformations

Hairy roots: Seeds of tomato (*Solanum* spp.) cv. Moneymaker were surface-sterilized in 70% ethanol for 10 min and in 3% NaOCl for 20 min (rinsing with sterile deionized water was performed in between the two sterilization steps), and then rinsed 3 times 5 min each with

568 sterile deionized water. The seeds were germinated on Murashige and Skoog (MS) tissue
569 culture medium [46] containing 4.3 g/L MS medium (Duchefa; catalog no. M0221.0050), 0.5
570 g/L MES, 20 g/L sucrose, pH 5.8, and 8 g/L agar (Difco; catalog no. 214530) in magenta boxes
571 (~50 ml). The pH of the medium was adjusted to 5.8 with KOH and autoclaved at 121°C for
572 20 min. The boxes were covered and placed in the dark at 4°C in a cold room for two days.
573 Subsequently, the boxes were transferred to a 24°C growth chamber (16 h light/8 h
574 photoperiod) for ~10 days until cotyledons were fully expanded and the true leaves just
575 emerged. Rhizogenic *Agrobacterium* (RAB) transformation was essentially performed as
576 described previously [47] with some minor modifications. More specifically, competent
577 rhizogenic *Agrobacterium* cells were transformed by electroporation (Shen and Forde 1989)
578 with the desired binary vector, plated on YEB medium plates with the appropriate antibiotics
579 (100 mg/L spectinomycin), and incubated for 3 to 4 d at 28°C. A transformed rhizogenic
580 *Agrobacterium* culture was inoculated from fresh plates into YEB liquid medium with the
581 appropriate antibiotics added and grown overnight at 28°C with shaking at 200 rpm. The RAB
582 culture was used to transform 20 to 40 tomato cotyledon halves. Using a scalpel, the cotyledons
583 were cut in half from ~10 days old tomato seedlings, transferred (adaxial side down) onto MS
584 liquid medium. The MS liquid was subsequently removed and the cotyledon halves
585 immediately immersed in a bacterial suspension at an optical density at 600 nm of 0.3 in MS
586 liquid medium for 20 min, then blotted on sterile Whatman filter paper and transferred (adaxial
587 side down) onto MS agar plates without antibiotics (4.3 g/L MS medium, 0.5 g/L MES, 30 g/L
588 sucrose, pH 5.8, and 8 g/L agar). The co-cultivation culture plates were closed with aeropore
589 tape. After 3 to 4 days of incubation at 22-25°C in the dark (Oberpichler, Rosen et al. 2008),
590 the cotyledons were transferred to MS agar plates with 200 mg/L cefotaxime (Duchefa;
591 catalogue no. c0111.0025) and 50 mg/L kanamycin and returned to 22-25°C. Typically, three
592 to five independent roots arise from each cotyledon. The expression of the eGFP marker of
593 antibiotic-resistant roots that emerged was monitored by means of fluorescent microscopic
594 imaging (Leica stereomicroscope and imaging DFC7000 T Leica microscope camera) and four
595 to ten independent roots showing expression of the marker were subcloned for each construct.
596 These roots were subsequently transferred to new selection plates with the same antibiotic
597 concentration for 3 rounds of subcultivation (~6 weeks) before antibiotics-free cultivation of
598 the hairy root cultures in liquid MS (in 50 ml Falcon tubes containing 10 to 30 ml MS medium
599 at 22-25°C and shaking at 300 rpm) and downstream analysis. After 3 rounds of cultivation,
600 root cultures were maintained and grown in antibiotics-free half-strength (½) Murashige and
601 Skoog (MS) medium supplemented with 3% sucrose at 22-25°C.

N. benthamiana: Wild-type tobacco (*Nicotiana benthamiana*) plants were grown under normal light and dark regime at 25°C and 70% relative humidity1. 3- to 4-weeks old *N. benthamiana* plants were watered from the bottom ~2h prior infiltration. Transformed *Agrobacterium tumefaciens* strain C58C1 Rif^R (pMP90), AGL1 Rif^R) or GV3101 Rif^R harbouring the constructs of interest were used to infiltrate tobacco leaves and used for transient expression of binary constructs by *Agrobacterium tumefaciens*-mediated transient transformation of lower epidermal leaf cells essentially as described previously [48]. Transformed *Agrobacterium tumefaciens* were grown for ~20h in a shaking incubator (200 rpm) at 28°C in 5 mL of LB-medium (Luria/Miller) (Carl Roth) or yeast extract broth (YEB) medium (5 g/L beef extract, 1 g/L yeast extract, 5 g/L peptone, 0.5 g/L $MgCl_2$, and 15 g/L bacterial agar), supplemented with appropriate antibiotics (i.e. 100 g/L spectinomycin). After incubation, the bacterial culture was transferred to 15 ml Falcon tubes and centrifuged (10 min, 5,000 rpm). The pellets were washed with 5 mL of the infiltration buffer (10 mM $MgCl_2$, 10 mM MES pH 5.7) and the final pellet resuspended in the infiltration buffer supplemented with 100-150 µM acetosyringone. The bacterial suspension was diluted with supplemented infiltration buffer to adjust the inoculum concentration to a final OD600 value of 0.025-1.0. The inoculum was incubated for 2-3 h at room temperature before injecting and delivered to tobacco by gentle pressure infiltration of the lower epidermis leaves (fourth and older true leaves were used; and about 4/5-1/1 of their full size) with a 1-mL hypodermic syringe without needle [49].

Arabidopsis cell suspension: The PSB-D Arabidopsis thaliana cell suspension cultures were transformed with the POI: 35sp::GFP/TPLATE/TML-BioID/BioID2, 35sp::TPLATE/TML-$(GGGGS)_{13}$ BioID/BioID2 and 35sp:: GFP/TPLATE-$(GGGGS)_{13}$ TurboID and selected without callus screening, grown and subcultured as described by [36].

Biotin treatments

Hairy roots: For assessing self-biotinylation, 2 weeks old 25 ml liquid cultures were added 5 ml fresh MS medium with or w/o supplemented biotin (i.e. 50 µM f.c.; stock solution dissolved in water) for 2h or 24h and samples collected. Two independent root cultures were analyzed per combination and the experiment repeated twice with similar results.

N. benthamiana leaves*:* Plants were kept under normal growing conditions 22°C, re-infiltrated with infiltration buffer (no biotin) or alternatively, infiltration buffer supplemented with biotin (stock solution dissolved in DMSO or water) and samples collected at the indicated times points. Two infiltrated tobacco leaf segments/leaves were analyzed per combination.

Arabidopsis cell cultures: were grown under normal conditions, at 25°C at 130 rpm in the dark. 48 h after subculturing, the required amount of biotin was added and the cell culture was transferred to the desired temperature for 24 h at 130 rpm in the dark in an INCLU-line IL56 (VWR) incubator. After 24 h, cell cultures were harvested and flash frozen in liquid nitrogen and stored at -70° till used.

Protein extractions

Hairy roots: The tissue samples were flash frozen and crushed using a liquid cooled mortar and pestle and the crushed material transferred to a 1.5 ml Eppendorf in homogenization buffer (25 mM Tris-HCl pH 7.6, 15 mM $MgCl_2$, 5 mM EGTA, 150 mM NaCl, 15mM $pNO_2PhenylPO_4$, 15 mM β-glycerolphosphate, 1mM DTT, 0.1% NP-40, 0.1 mM Na_3VO_4, 1mM NaF, 1mM PMSF, 10 µg/ml leupeptin, 10 µg/ml aprotinin, 10 µg/ml SBTI, 0.1 mM benzamidine, 5 µg/ml antipain, 5 µg/ml pepstatin, 5 µg/ml chymostatin, 1µM E64, 5% ethylene glycol) was added with volumes according to the dry weight of the recovered material (1/1 w/v) and protein material extracted by three repetitive freeze-thaw cycles in liquid nitrogen and the lysate transferred to a 1.5 ml Eppendorf. The lysates were cleared by centrifugation for 15 min at 16,100 x g (4 °C) and the supernatant transferred to a new 1.5 ml Eppendorf. This step was repeated two times and the protein concentration was determined by the DC Protein Assay Kit (Bio-Rad, Munich, Germany) according to the manufacturer's instructions.

N. benthamiana leaves*:* The tissue samples were crushed using a liquid cooled mortar and pestle and the crushed material transferred to a 1.5 ml Eppendorf in homogenization buffer. Leaves were harvested and directly frozen in liquid nitrogen. Proteins were extracted with buffer containing 50 mM Tris-HCl (pH 7.5), 150 mM NaCl, 10 % glycerol, 2 mM EDTA, 5 mM DTT, 1 mM PMSF, Protease inhibitor Cocktail (Roche) and 1 % (v/v) IGEPAL CA-630 (Sigma-Aldrich). Extraction buffer was added at 2 ml/g tissue. Extracts were incubated at 4 °C for 1 h and then centrifuged at 4 °C, 13000 rpm for 30min. Supernatants were used directly or filtered through PD-10 columns (GE Healthcare) and incubated with streptavidin (Roche) or GFP (Chromotek) beads for 1 h. For ammonium acetate protein precipitation, supernatants were precipitated using 5x v/v pre-cold 0.1 M ammonium acetate in methanol at -20 °C for 2h and then centrifuged at 4 °C, 13,000 rpm for 15min. The pellet was washed with pre-cold 0.1 M ammonium acetate and dissolved in the same extraction buffer plus 1% SDS. Magnetic separation was done using Dynabeads™ M-280 Streptavidin (Thermo Fisher Scientific) followed by 5 times washing in buffer containing 50 mM Tris-HCl (pH 7.5), 150 mM NaCl,

10 % glycerol, 2 mM EDTA, Protease inhibitor Cocktail (Roche) and 0.5 % (v/v) IGEPAL CA-630 (Sigma-Aldrich) and one time in buffer containing 50 mM Tris-HCl (pH 7.5), 1M NaCl, 10 % glycerol, 2 mM EDTA, Protease inhibitor Cocktail (Roche) and 0.5 % (v/v) IGEPAL CA-630 (Sigma-Aldrich) at 4°C. To release the proteins, 100 µl 2x NuPAGE LDS sample buffer (Invitrogen) was added and samples were heated for 5 min at 95 °C

Arabidopsis cell cultures: Total protein extracts were obtained from liquid nitrogen retched (20 Hz, 1 min), biotin treated and harvested, *Arabidopsis* cell suspension cultures using double the volume (w/2v) of extraction buffer containing 150mM Tris-HCl pH 7.5; 150 mM NaCl; 10 % glycerol; 10 mM EDTA; 1mM sodium molybdate; 1 mM NaF and freshly added 10 mM DTT; 1 % (v/v) protease inhibitor cocktail (P9599, Sigma (1 tablet/10ml elution buffer) and 1 % (v/v) NP-40. Cell debris was removed by two rounds of centrifugation at 14,000 rpm for 20 min at 4°C and the supernatant was collected.

SDS-PAGE and western blots

Hairy roots: Sample loading buffer was added and equivalent amounts of protein (~ 30 µg) separated by SDS-PAGE (1.0 mm thick 4 to 12% polyacrylamide Criterion Bis-Tris XT- gels, Bio-Rad or equivalent) in MOPS buffer (Bio-Rad) at 150 V. Subsequently, proteins were transferred onto PVDF membranes with 0.2 um porous size. Membranes were blocked for 30 min in a 1:1 Tris-buffered saline (TBS)/Odyssey Blocking solution (cat n° 927-40003, LI-COR, Lincoln, NE, USA) and probed by Western blotting. Following overnight incubation of primary antibody in TBS-T/Odyssey blocking buffer and three 10 min washes in TBS-T (0.1% Tween-20), membranes were incubated with secondary antibody for 30 min in TBS-T/Odyssey blocking buffer followed by 3 washes in TBS-T or TBS (last wash step). The following antibodies were used: streptavidin-S680 (Invitrogen, S32358, 1/10000), mouse anti-Flag (Sigma, F3165; 1/5000), mouse anti-actin (plant) (Sigma, A0480, 1/2000), rabbit anti-GFP (Invitrogen, A11122, 1/1000), anti-mouse (IRDye 800 CW goat anti-mouse antibody IgG, LI-COR, cat n° 926-32210, 1/10000) and anti-rabbit (IRDye 800 CW goat anti-rabbit IgG, LI-COR, cat n° 926-3221, 1/10000). The bands were visualized using an Odyssey infrared imaging system (LI-COR) and the intensity of bands assessed using the LICOR Odyssey software for Western Blot image processing.

N. benthamiana: Extracted proteins were loaded to 12% SDS-PAGE gels and separated for 2 h at 90-110V. SDS-PAGE gels were blotted via wet transfer on PVDF membranes (Carl Roth) overnight at 30V. Membrane blocking was performed with 3%BSA in PBS-t buffer for 1 h at

699 room temperature followed by incubation with Mouse-anti-GFP (TaKaRa) (1/5,000) for 2 h
700 followed by Anti-Mouse-HRP (Sigma-Aldrich) (1/5,000) for 2 h or directly Strep-Tactin-HRP
701 (iba-Life Sciences) (1/5,000) for 2 h. Chemiluminescence was detected with Clarity Western
702 ECL (Bio-rad).

703 *N. benthamiana:* Input and eluted proteins were loaded to 12% SDS-PAGE gels and separated
704 for 1-2 h at 120 V. SDS-PAGE gels were blotted via wet transfer on PVDF membranes (Bio-
705 rad) 3h at 300 mA in a cool room. The membrane was blocked with 3% BSA in PBS-T buffer
706 for 1 h at room temperature followed by incubation with Streptavidin-HRP (Sigma-Aldrich)
707 (1/25,000) for 2 h. Chemiluminescence was detected with ECL Prime Western Blotting
708 Detection Reagent (GE healthcare).

709 *Arabidopsis cell cultures:* The extracts were heated in sample buffer for 10 min at 70°C and
710 loaded in equal amounts (20 µg) on a 4-20% SDS-PAGE gel. SDS-PAGE separated proteins
711 were blotted on PVDF membrane (Thermo Fischer). Membranes were blocked overnight at
712 RT in 5% (v/v) BSA dissolved in 25 mM Tris-HCl, pH8, 150 mM NaCl and 0.1% Tween20.
713 The blots were then incubated at room temperature with the Pierce High Sensitivity
714 Streptavidin-HRP Thermo Fisher scientific (1/2,000) or Abcam Anti-HA-HRP tag antibody
715 (ab1190) (1/5,000) for 2 h. Antigen-antibody complexes were detected using
716 chemiluminescence (Perkin-Elmer).
717
718 ***Protein Extraction and Pull-Down for mass spectrometry analysis***
719 Arabidopsis cell cultures expressing different POI were ground in 0.67 volume of extraction
720 buffer containing 100mM Tris (pH7.5), 2% SDS and 8M Urea. The extract was mechanically
721 disrupted using three repetitive freeze-thaw cycles followed by 2 cycles of sonication at output
722 level 4 with a 40% duty cycle for 50 secs. Cell debris was removed by two rounds of
723 centrifugation at 20,000 rpm for 20 min and the supernatant was buffer exchanged using pre-
724 equilibrated PD-10 columns and eluted in binding buffer containing 100mM Tris (pH7.5), 2%
725 SDS and 7.5M Urea. Pull-downs were performed in triplicate. For each pull-down, 1/3 of the
726 soluble protein extract was incubated with 200 µl slurry of streptavidin sepharose high-
727 performance beads (Amersham) overnight on a rotating wheel at RT. The unbound fraction
728 was removed after brief centrifugation at 1,500 rpm for 1 min. Beads were transferred to a
729 Mobicol column and washed with 4 ml binding buffer incubating for 5 min, followed by a wash
730 with high salt buffer containing 1M NaCl, 100 mM Tris-HCl pH 7.5 and incubated for 30 min.
731 The beads were washed once with ultrapure water, incubated for five min, and finally washed

with 3.2ml of 50mM ammonium bicarbonate pH8.0. Proteins were digested on beads with Trypsin/LysC (Promega) overnight followed by zip-tip cleanup using C-18 Omix tips (Agilent). Digests containing the unbiotinylated peptides were dried in a Speedvac and stored at -20 °C until LC-MS/MS analyses. Biotinylated peptides were eluted first by adding 300µl of the elution buffer (0.2% TFA, 0.1% formic acid and 80% acetonitrile in water) [29] and collecting the eluted proteins by centrifuging at 1500 rpm for 1 min and a second elution by adding 300µl of the elution buffer and heating at 95°C for 5 min for maximum release of peptides. A short spin at 1500 rpm for 1 min was done to collect the eluted peptides. The two elutes were pooled together and dried in a Speedvac. The dried peptides were dissolved in 1% TFA solution to perform zip-tip cleanup using C-18 Omix tips (Agilent). Digests were dried in a Speedvac as Elution-2 and stored at -20 °C until LC-MS/MS analysis.

Mass Spectrometry and Data Analysis

Pull-down experiments were analyzed on a Q Exactive (ThermoFisher Scientific) as previously reported [50]. Proteins were identified with MaxQuant using standard parameters. The relative abundance of the TPC subunits in pull-down and BioID experiments was determined by average LFQ intensities of the TPC subunits per set of three experiments, normalized versus the bait, TPLATE or TML, and taking into account the MW of the TPC subunit. LFQ values in case of non-detection were imputed using the Perseus software package. For each of the TPC subunits, the identified peptides were mapped to the protein sequence. Non-biotinylated and biotinylated peptides of TPC subunits were mapped to the protein sequence by using the Draw Map tool in the MSTools package (http://peterslab.org/MSTools/ [51]) and put together using Inkscape v 0.92.4 (www.inkscape.org). Domain annotation of TPC subunits was retrieved using InterPro protein sequence analysis (https://www.ebi.ac.uk/interpro/) [52].

REFERENCES

1. Varnaite, R. and S.A. MacNeill, *Meet the neighbors: Mapping local protein interactomes by proximity-dependent labeling with BioID.* Proteomics, 2016. **16**(19): p. 2503-2518.
2. van Steensel, B. and S. Henikoff, *Identification of in vivo DNA targets of chromatin proteins using tethered dam methyltransferase.* Nat Biotechnol, 2000. **18**(4): p. 424-8.
3. Kim, D.I. and K.J. Roux, *Filling the Void: Proximity-Based Labeling of Proteins in Living Cells.* Trends Cell Biol, 2016. **26**(11): p. 804-817.
4. Choi-Rhee, E., H. Schulman, and J.E. Cronan, *Promiscuous protein biotinylation by Escherichia coli biotin protein ligase.* Protein Sci, 2004. **13**(11): p. 3043-50.
5. Roux, K.J., et al., *A promiscuous biotin ligase fusion protein identifies proximal and interacting proteins in mammalian cells.* J Cell Biol, 2012. **196**(6): p. 801-10.

6. Kwon, K. and D. Beckett, *Function of a conserved sequence motif in biotin holoenzyme synthetases.* Protein Sci, 2000. **9**(8): p. 1530-9.
7. Cronan, J.E., *Targeted and proximity-dependent promiscuous protein biotinylation by a mutant Escherichia coli biotin protein ligase.* J Nutr Biochem, 2005. **16**(7): p. 416-8.
8. Kim, D.I., et al., *An improved smaller biotin ligase for BioID proximity labeling.* Mol Biol Cell, 2016. **27**(8): p. 1188-96.
9. Branon, T.C., et al., *Efficient proximity labeling in living cells and organisms with TurboID.* Nat Biotechnol, 2018. **36**(9): p. 880-887.
10. Kim, D.I., et al., *Probing nuclear pore complex architecture with proximity-dependent biotinylation.* Proc Natl Acad Sci U S A, 2014. **111**(24): p. E2453-61.
11. Opitz, N., et al., *Capturing the Asc1p/Receptor for Activated C Kinase 1 (RACK1) Microenvironment at the Head Region of the 40S Ribosome with Quantitative BioID in Yeast.* Mol Cell Proteomics, 2017. **16**(12): p. 2199-2218.
12. Opitz, N., et al., *Capturing the Asc1p/Receptor for Activated C Kinase 1 (RACK1) Microenvironment at the Head Region of the 40S Ribosome with Quantitative BioID in Yeast.* Molecular & Cellular Proteomics, 2017. **16**(12): p. 2199-2218.
13. Batsios, P., I. Meyer, and R. Graf, *Proximity-Dependent Biotin Identification (BioID) in Dictyostelium Amoebae.* Methods Enzymol, 2016. **569**: p. 23-42.
14. Gu, B., et al., *AIRE is a critical spindle-associated protein in embryonic stem cells.* Elife, 2017. **6**.
15. Dingar, D., et al., *BioID identifies novel c-MYC interacting partners in cultured cells and xenograft tumors.* J Proteomics, 2015. **118**: p. 95-111.
16. Gupta, G.D., et al., *A Dynamic Protein Interaction Landscape of the Human Centrosome-Cilium Interface.* Cell, 2015. **163**(6): p. 1484-99.
17. Youn, J.Y., et al., *High-Density Proximity Mapping Reveals the Subcellular Organization of mRNA-Associated Granules and Bodies.* Mol Cell, 2018. **69**(3): p. 517-532.e11.
18. Lin, Q., et al., *Screening of Proximal and Interacting Proteins in Rice Protoplasts by Proximity-Dependent Biotinylation.* Front Plant Sci, 2017. **8**: p. 749.
19. Conlan, B., et al., *Development of a Rapid in planta BioID System as a Probe for Plasma Membrane-Associated Immunity Proteins.* Frontiers in plant science, 2018. **9**: p. 1882-1882.
20. Khan, M., et al., *In planta proximity dependent biotin identification (BioID).* Scientific Reports, 2018. **8**(1): p. 9212.
21. Das, P.P., et al., *In planta proximity-dependent biotin identification (BioID) identifies a TMV replication co-chaperone NbSGT1 in the vicinity of 126 kDa replicase.* Journal of Proteomics, 2019. **204**: p. 103402.
22. Alban, C., D. Job, and R. Douce, *BIOTIN METABOLISM IN PLANTS.* Annu Rev Plant Physiol Plant Mol Biol, 2000. **51**: p. 17-47.
23. Pirner, H.M. and J. Stolz, *Biotin sensing in Saccharomyces cerevisiae is mediated by a conserved DNA element and requires the activity of biotin-protein ligase.* Journal of Biological Chemistry, 2006. **281**(18): p. 12381-12389.
24. Ried, M.K., M. Antolin-Llovera, and M. Parniske, *Spontaneous symbiotic reprogramming of plant roots triggered by receptor-like kinases.* Elife, 2014. **3**.
25. Antolin-Llovera, M., M.K. Ried, and M. Parniske, *Cleavage of the SYMBIOSIS RECEPTOR-LIKE KINASE ectodomain promotes complex formation with Nod factor receptor 5.* Curr Biol, 2014. **24**(4): p. 422-7.
26. Grebe, M., et al., *Arabidopsis sterol endocytosis involves actin-mediated trafficking via ARA6-positive early endosomes.* Curr Biol, 2003. **13**(16): p. 1378-87.
27. Gadeyne, A., et al., *The TPLATE adaptor complex drives clathrin-mediated endocytosis in plants.* Cell, 2014. **156**(4): p. 691-704.

28. Cox, J., et al., *Accurate proteome-wide label-free quantification by delayed normalization and maximal peptide ratio extraction, termed MaxLFQ.* Mol Cell Proteomics, 2014. **13**(9): p. 2513-26.
29. Schiapparelli, L.M., et al., *Direct detection of biotinylated proteins by mass spectrometry.* J Proteome Res, 2014. **13**(9): p. 3966-78.
30. Deal, R.B. and S. Henikoff, *The INTACT method for cell type-specific gene expression and chromatin profiling in Arabidopsis thaliana.* Nat Protoc, 2011. **6**(1): p. 56-68.
31. Beckett, D., E. Kovaleva, and P.J. Schatz, *A minimal peptide substrate in biotin holoenzyme synthetase-catalyzed biotinylation.* Protein Sci, 1999. **8**(4): p. 921-9.
32. Mair, A., et al., *Proximity labeling of protein complexes and cell type-specific organellar proteomes in Arabidopsis enabled by TurboID.* BioRxiv 2019: p. 629675.
33. Kim, T.-W., et al., *Application of TurboID-mediated proximity labeling for mapping a GSK3 kinase signaling network in Arabidopsis.* BioRxiv 2019: p. 636324.
34. Ashby, A.M., et al., *Ti plasmid-specified chemotaxis of Agrobacterium tumefaciens C58C1 toward vir-inducing phenolic compounds and soluble factors from monocotyledonous and dicotyledonous plants.* J Bacteriol, 1988. **170**(9): p. 4181-7.
35. Kajala, K., D.A. Coil, and S.M. Brady, *Draft Genome Sequence of Rhizobium rhizogenes Strain ATCC 15834.* Genome Announc, 2014. **2**(5).
36. Van Leene, J., et al., *A tandem affinity purification-based technology platform to study the cell cycle interactome in Arabidopsis thaliana.* Mol Cell Proteomics, 2007. **6**(7): p. 1226-38.
37. Karimi, M., et al., *Building Blocks for Plant Gene Assembly.* 2007. **145**(4): p. 1183-1191.
38. Patron, N.J., et al., *Standards for plant synthetic biology: a common syntax for exchange of DNA parts.* New Phytol, 2015. **208**(1): p. 13-9.
39. Binder, A., et al., *A Modular Plasmid Assembly Kit for Multigene Expression, Gene Silencing and Silencing Rescue in Plants.* PLOS ONE, 2014. **9**(2): p. e88218.
40. Schwessinger, B., et al., *Phosphorylation-Dependent Differential Regulation of Plant Growth, Cell Death, and Innate Immunity by the Regulatory Receptor-Like Kinase BAK1.* PLOS Genetics, 2011. **7**(4): p. e1002046.
41. Madsen, E.B., et al., *Autophosphorylation is essential for the in vivo function of the Lotus japonicus Nod factor receptor 1 and receptor-mediated signalling in cooperation with Nod factor receptor 5.* Plant J, 2011. **65**(3): p. 404-17.
42. Wong, J., et al., *A Lotus japonicus cytoplasmic kinase connects Nod factor perception by the NFR5 LysM receptor to nodulation.* Proc Natl Acad Sci U S A, 2019.
43. Karimi, M., B. De Meyer, and P. Hilson, *Modular cloning in plant cells.* Trends Plant Sci, 2005. **10**(3): p. 103-5.
44. Mylle, E., et al., *Emission spectra profiling of fluorescent proteins in living plant cells.* 2013. **9**(1): p. 10.
45. Van Damme, D., et al., *Somatic Cytokinesis and Pollen Maturation in Arabidopsis Depend on TPLATE, Which Has Domains Similar to Coat Proteins.* 2006. **18**(12): p. 3502-3518.
46. Murashige, T. and F. Skoog, *A Revised Medium for Rapid Growth and Bio Assays with Tobacco Tissue Cultures.* Physiologia Plantarum, 1962. **15**(3): p. 473-497.
47. Harvey, J.J.W., J.E. Lincoln, and D.G. Gilchrist, *Programmed cell death suppression in transformed plant tissue by tomato cDNAs identified from an Agrobacterium rhizogenes-based functional screen.* Molecular Genetics and Genomics, 2008. **279**(5): p. 509-521.
48. Boruc, J., et al., *Functional modules in the Arabidopsis core cell cycle binary protein-protein interaction network.* Plant Cell, 2010. **22**(4): p. 1264-80.
49. Moschou, P.N., et al., *Separase Promotes Microtubule Polymerization by Activating CENP-E-Related Kinesin Kin7.* Dev Cell, 2016. **37**(4): p. 350-361.
50. Nelissen, H., et al., *Dynamic Changes in ANGUSTIFOLIA3 Complex Composition Reveal a Growth Regulatory Mechanism in the Maize Leaf.* Plant Cell, 2015. **27**(6): p. 1605-19.

867 51. Kavan, D. and P. Man, *MSTools—Web based application for visualization and presentation of*
868 *HXMS data.* International Journal of Mass Spectrometry, 2011. **302**(1): p. 53-58.
869 52. Mitchell, A.L., et al., *InterPro in 2019: improving coverage, classification and access to*
870 *protein sequence annotations.* Nucleic Acids Research, 2018. **47**(D1): p. D351-D360.
871

872